



---

MSU Graduate Theses

---

Summer 2024

## Carbaryl-Induced Leaf Necrosis in *Vitis Rupestris* B-38


Courtney Nicole Duncan

Missouri State University, [Duncan103@live.missouristate.edu](mailto:Duncan103@live.missouristate.edu)

As with any intellectual project, the content and views expressed in this thesis may be considered objectionable by some readers. However, this student-scholar's work has been judged to have academic value by the student's thesis committee members trained in the discipline. The content and views expressed in this thesis are those of the student-scholar and are not endorsed by Missouri State University, its Graduate College, or its employees.

---

Follow this and additional works at: <https://bearworks.missouristate.edu/theses>

 Part of the [Biology Commons](#), [Genetics and Genomics Commons](#), [Plant Sciences Commons](#), and the [Viticulture and Oenology Commons](#)

### Recommended Citation

Duncan, Courtney Nicole, "Carbaryl-Induced Leaf Necrosis in *Vitis Rupestris* B-38" (2024). *MSU Graduate Theses*. 3977.

<https://bearworks.missouristate.edu/theses/3977>

This article or document was made available through BearWorks, the institutional repository of Missouri State University. The work contained in it may be protected by copyright and require permission of the copyright holder for reuse or redistribution.

For more information, please contact [bearworks@missouristate.edu](mailto:bearworks@missouristate.edu).

**CARBARYL-INDUCED LEAF NECROSIS IN *VITIS RUPESTRIS* B-38**

A Master's Thesis

Presented to

The Graduate College of

Missouri State University

In Partial Fulfillment

Of the Requirements for the Degree

Master of Science, Biology

By

Courtney Duncan

August 2024

Copyright 2024 by Courtney Duncan

# CARBARYL-INDUCED LEAF NECROSIS IN *VITIS RUPESTRIS* B-38

Biology

Missouri State University, August 2024

Master of Science

Courtney Duncan

## ABSTRACT

Agricultural insecticides are formulated to target insects while minimizing harm to the intended crop. In rare instances, however, insecticides induce harmful physiological reactions in certain plant genomes, inflicting severe tissue damage. This project investigated the genetic basis of such a reaction observed in the grape genotype *Vitis rupestris* B38 following exposure to the insecticide carbaryl, which manifests as interveinal leaf necrosis. Through analysis of an F1 hybrid progeny of this grapevine, I mapped this phenotype to a QTL on chromosome 16. The carbaryl-sensitive trait was repeatedly mapped to the same locus using phenotype data from two different field locations and from an *in vitro* bioassay. RNA-seq and gene ontology enrichment analyses revealed the activation of various defense- and stress-related mechanisms, and strongly suggested the involvement of salicylic acid- and jasmonic acid-dependent defense responses. The RNA-seq data suggested a misdirected hypersensitive response (HR) in sensitive plants; differentially expressed genes (DEGs) associated with plant pathogen defense pathways further support this speculation. However, RT-qPCR analysis of *NDRI/HINI-like protein 6* gene expression did not validate the involvement of such pathways, therefore, further molecular analysis is needed to fully elucidate the underlying mechanisms of carbaryl sensitivity. Altogether, the findings of this thesis highlight the intricate interplay of plant defense pathways in response to xenobiotic stressors and emphasize the ecological significance of plant-insecticide interactions.

**KEYWORDS:** carbaryl, interveinal necrosis, *Vitis rupestris*, RNA-seq analysis, QTL, F1 hybrid progeny, RT-qPCR, hypersensitive response

**CARBARYL-INDUCED LEAF NECROSIS IN *VITIS RUPESTRIS* B-38**

By

Courtney Duncan

A Master's Thesis  
Submitted to the Graduate College  
Of Missouri State University  
In Partial Fulfillment of the Requirements  
For the Degree of Master of Science, Biology

August 2024

Approved:

Laszlo G. Kovacs, Ph.D., Thesis Committee Chair

D. Alexander Wait, Ph.D., Committee Member

Jay P. McEntee, Ph.D., Committee Member

Julie J. Masterson, Ph.D., Dean of the Graduate College

In the interest of academic freedom and the principle of free speech, approval of this thesis indicates the format is acceptable and meets the academic criteria for the discipline as determined by the faculty that constitute the thesis committee. The content and views expressed in this thesis are those of the student-scholar and are not endorsed by Missouri State University, its Graduate college, or its employees.

## ACKNOWLEDGEMENTS

I would like to thank my undergraduate and thesis advisor Dr. Laszlo G. Kovacs for the opportunity to conduct undergraduate and graduate research, and for providing guidance throughout my studies. I am also grateful to my thesis committee members Dr. Jay P. McEntee and Dr. Alexander D. Wait for the constructive feedback provided to my thesis research. I wish to express my gratitude to the Graduate College and Department of Biology at Missouri State University. I thank Dr. Courtney Coleman, Dr. Jason Londo, Danielle Evilsizor, Michael Bigelow, Katelin Meek, and others for their help throughout my research.

I dedicate this thesis to my family, for their continued support and encouragement throughout my education.

## TABLE OF CONTENTS

Overview	Page 1
Introduction	Page 2
Chemical Pest Control	Page 2
Carbaryl as an Insecticide	Page 4
Insecticides that Damage Plants	Page 7
Methods	Page 9
Plant Material	Page 9
Phenotyping NY and MO Vineyards	Page 9
<i>In Vitro</i> Leaf Disk Bioassay	Page 10
Scoring of <i>In Vitro</i> Leaf Disks	Page 11
QTL Mapping	Page 11
RNA Extraction and RNA-seq Analysis	Page 12
Validation of RNA-seq Results Using RT-qPCR	Page 13
Results	Page 14
Symptoms and Segregation of Interveinal Necrosis in NY and MO	Page 14
QTL Mapping Based on NY and MO Field Data	Page 15
QTL Mapping Based on the <i>In Vitro</i> Leaf Disk Bioassay	Page 16
Gene Content of the QTL Region	Page 17
RNA-seq Analysis in Carbaryl-Treated Sensitive and Insensitive Plants	Page 17
Defense Genes of Interest Identified by RNA-seq Analysis	Page 19
Validation Using RT-qPCR	Page 21
Discussion	Page 21
Evidence of Insecticide Sensitivity in Grapevine	Page 21
RNA-seq Analysis in Carbaryl-Treated Sensitive and Insensitive Plants	Page 22
<i>EDS1</i> and <i>SAG101</i>	Page 23
<i>NHL</i> Genes and Salicylic Acid Biosynthesis	Page 24
<i>WRKY</i> Transcription Factors, <i>JOX</i> , and <i>ERF.C.3</i>	Page 26
Cross-Talk Between Salicylic Acid- and Jasmonic Acid-Mediated Pathways	Page 27
References	Page 30

## ABBREVIATIONS

QTL	Quantitative Trait Locus
HR	Hypersensitive Response
DEGs	Differentially Expressed Genes
EPA	Environmental Protection Agency
AChE	Acetylcholinesterase
RT-qPCR	Real-Time Quantitative PCR
NY	Geneva, New York, USA
MO	Springfield, Missouri, USA
SE	Sensitive
IN	Insensitive
RPKM	Reads Per Kilobase Per Million Reads
C <sub>t</sub>	Cycle Threshold
hpt	Hours Post-Treatment
LOD	Logarithm of Odds
SA	Salicylic Acid
JA	Jasmonic Acid
ETH	Ethylene
GO	Gene Ontology
EDS1	Enhanced Disease Susceptibility 1
SAG101	Senescence-Associated Gene 101
NHL6	NDR1/HIN1-Like Protein 6
JOX	Jasmonate-Induced Oxygenase 1
ERF.C3	Ethylene-Response Transcription Factor C3
NBS-LRR	Nucleotide Binding Site, Leucine-Rich Repeats
ETI	Effector-Triggered Immunity
ICS	Isochorismate Synthase
R	Resistance
PR	Pathogenesis-Related



## LIST OF TABLES

Table 1. Major types of insecticides	Page 39
Table 2. Scale used to score leaf disks <i>in vitro</i>	Page 40
Table 3. Individual plants used for RT-qPCR	Page 41
Table 4. Number of Reads Identified by RNA-seq Analysis	Page 42
Table 5. Number of up or downregulated genes in IN and SE plants at each time point	Page 43
Table 6. Genes of interest determined by RNA-seq analysis	Page 44

## LIST OF FIGURES

Figure 1. Molecular structures of carbaryl, methomyl, and fenthion	Page 45
Figure 2. Representative leaf disks for each <i>in vitro</i> carbaryl sensitivity score	Page 46
Figure 3. Examples of necrotic phenotype in IN and SE leaves following 50x carbaryl application in the greenhouse	Page 47
Figure 4. Example of necrotic phenotype in SE leaf following standard application in the field	Page 48
Figure 5. Segregation of the carbaryl sensitivity phenotype in different environments	Page 49
Figure 6. QTL and LOD graphs of the carbaryl-sensitivity allele according to field phenotyping	Page 50
Figure 7. QTL and LOD graphs of the carbaryl-sensitivity allele according to <i>in vitro</i> bioassay	Page 51
Figure 8. <i>In vitro</i> leaf disk bioassay scores plotted against frequency of occurrence	Page 52
Figure 9. Number of carbaryl-responsive genes unique to and shared between SE and IN vines	Page 53
Figure 10. Genes of interest as determined by RNA-seq analysis	Page 54
Figure 11. Gene ontology enrichment analysis of genes of interest	Page 55
Figure 12. Expression of <i>EDS1</i> and <i>SAG101</i>	Page 56
Figure 13. Expression of <i>trans-resveratrol di-O-methyltransferase</i> and <i>stilbene synthase 2</i>	Page 57
Figure 14. Expression of <i>NDR1/HIN1-like protein 6</i>	Page 58
Figure 15. Expression of <i>ethylene-response factor C3</i> and <i>jasmonate-induced oxygenase 1</i>	Page 59
Figure 16. Expression of <i>NDR1/HIN1-like protein6</i> measured by RT-qPCR	Page 60

## OVERVIEW

Despite efforts to limit chemical pesticides, their use continues, and unintended harm to non-target organisms remains a significant concern. Carbaryl is the fifth most common active ingredient in pesticide products and is primarily utilized as an insecticide in vineyards and orchards (US Geological Survey 2024, Atwood and Paisley-Jones 2017). According to EPA regulations, carbaryl is permissible in the United States and remains the third most-used insecticide across home gardens and commercial agriculture (EPA 2004). However, carbaryl is the second most frequent insecticide found in off-target water sources (Hoffman et al. 2000). It is considered toxic to vertebrates and invertebrates, humans included; thus, its use is prohibited in countries of the European Union (EPA 2004).

In rare instances, chemical insecticides have been shown to cause damage to plants (Ennis 1948, Lichtenstein et al. 1962). Here, I aim to address the inadequately acknowledged and insufficiently documented prevalence of plant-insecticide interactions. This work investigated the severe damage that occurs following carbaryl application to *V. rupestris* B-38, a genotype commonly used as a resource for disease-resistance breeding, and its progeny. I have identified several genes that suggest a hypersensitive defense-like response in a subset of F1 hybrids, induced specifically following the application of carbaryl insecticide. This response may provide insight into pathogen and xenobiotic defense mechanisms and the underlying implications of insecticide damage in plants. Understanding such interactions is crucial for mitigating the ecological harm of chemical pest control and ensuring effective crop management practices.

## INTRODUCTION

### Chemical Pest Control

Pest management is pivotal in agricultural practices, safeguarding crops against destructive insects, herbivores, fungi, and bacteria. Chemical pesticide use, specifically, has revolutionized the economic efficiency of crop management. However, the unintended consequences of chemical use extend far beyond targeted pests, inducing harm to beneficial insects and plants. Recent studies have shed light on the adverse effects of broad-range insecticides on various crops, ranging from reduced yields to disruptions in development-related metabolism (Giménez-Moolhuyzen et al. 2020). Further understanding of insecticide-induced damage to plants is critical for mitigating unintended ecological harm while ensuring productive crop protection strategies. Here, I investigate the specific case of carbaryl-induced sensitivity in *Vitis*.

Pest management practices have evolved alongside the advancement of agricultural societies, with evidence of their existence tracing back to at least 4,500 years ago. The first recorded example is from Samaria, where sulfur was rubbed on the skin to deter insects (Polyrakis 2009). During the same period, agricultural communities began to employ cultural techniques for control such as strategically adjusting the planting and harvesting times to avoid pest damage. In ancient Egypt, the medical document known as “Ebers papyrus” reported about 800 recipes, many of which included substances that acted as pesticides. The Chinese adopted such practices circa 1200 BC, using chemical agents to control agricultural pests: mercury- and arsenic-containing substances were used to control human lice outbreaks (Tudi et al. 2021). During the Middle Ages, biological methods were mainly used to control pests: rotenone and pyrethrum flowers were common household pest deterrents (Babinska et al. 2010, Tudi et al.

2021). The latter led to the development of organic pyrethroids, a class of insecticides commonly known for their use in mosquito control (Liu et al. 2006). Through the Enlightenment era, knowledge pertaining to pest control steadily increased. Handbooks containing pest control remedies were distributed throughout the general population and sulfur, mercury, and lead (among other inorganic compounds) were commercialized as means for eliminating pests (Benheim et al. 2012, Hassan 2019). The production of modern inorganic pesticides was also first seen in the mid-19<sup>th</sup> century. Copper sulfate, a fungicide first introduced in France during the 1830s, is still utilized as an effective tool against downy mildew in vineyards (Johnson 1935).

However, many harmful chemical products were introduced during this timeframe, with little awareness for their potential health and environmental effects. “Paris green” (copper (II) acetoarsenite) was first used in 1858 to control Colorado beetles – it also had a burning effect on leaves and caused toxicity to humans. Carbon disulfide was used on grapevines in Europe during the 1860s to fumigate roots against grape phylloxera but was soon replaced by biocontrol methods such as grafting on phylloxera-resistant rootstocks (Weber et al. 1996). The 1939 discovery of dichlorodiphenyltrichloroethane (DDT), used to control plant pests and malaria- and typhus-transmitting insects, revolutionized how the agriculture industry viewed and utilized chemical insecticides. It was not until decades later that the consequences of DDT application surfaced: due to its persistence in the environment, the compound affected entire ecosystems, including bird and fish fertility and hormonal effects in mammals (Carson 2002). Nonetheless, the introduction of DDT began the widespread use of a broad variety of synthetic organic compounds for pest control; Dinitro-ortho-cresol (DNOC) (1892), phenolic acids such as 2,4-D (1944), MCPA (1947), atrazine (1957), and glyphosate (1974) were introduced as herbicides. In

1943, German chemists synthesized parathion, the first phosphoroorganic insecticide. Carbaryl, the first carbamin insecticide, was synthesized in Ciba-Geigy laboratories in 1950 (Babinska et al. 2010). This evolution of new chemical agents extends into today's thriving market of commercialized pesticides. Within the last century, several large manufacturing giants have established themselves as leaders in pesticide production and patenting; Bayer CropScience®, DuPont® (an associated branch of Corteva®), and Syngenta® are among the top patent publishers and producers of pesticides (Umetsu and Shirai 2020).

Chemical insecticides are categorized by their mode of action. Many act by interfering with the normal function of the insect's nervous system, while others act as growth regulators or endotoxins. The major classes of insecticides are organophosphates, carbamates, nicotinoids, butenolides, and spinosyns. A complete list of insecticide categories, their mode of action, and target organisms are shown in **Table 1**. The use of dinitrophenol and quinazoline insecticides has been discontinued in agriculture because of their toxicity to humans (Radcliffe et al. 2009, EPA 2015a).

### **Carbaryl as an Insecticide**

Carbaryl, a member of the carbamate family, is the fifth most common active ingredient in pesticide products (Atwood and Paisley-Jones 2017). Carbaryl is a relatively low-cost option for pest control, and its ability to readily decompose in sunlight within two to four days makes it suitable for field use (Carbaryl 1994). It is primarily utilized as an insecticide in orchards and vineyards (Estimated Annual Agricultural Pesticide Use 2024). Annual application has been reported in over 140 crops (Pesticide Factsheets); in 2016, it was the active compound in more than 190 registered products (Bond et al. 2016). From 2013 to 2017, the EPA reported an

average of 700,000 pounds applied to over 650,000 acres of crops annually, with an additional 2 million pounds applied to non-agricultural sites such as infrastructure (buildings and roadways) and landscape (ornamentals and turf) (Paisley-Jones 2020).

Carbaryl was first commercially introduced by Union Carbide (Aventis CropScience®) in the 1950s and has recently been sold under the brand name Sevin®. Carbaryl-containing products are authorized to be applied to a broad range of crops. The Organisation for Economic Co-operation and Development (OECD) permits the use of carbaryl in some of its 38 countries, including the United States, Australia, and New Zealand (Re-evaluation Decision RVD2016-02 2016). The specific carbaryl formulation labeled for use in grapevine is marketed in the United States under the brand name Sevin SL. It is recommended for the control of flea beetles, grape leafhopper, grape leafroller, leafhoppers, Japanese beetles, June beetles, grape berry moths, and cutworms (Radcliffe et al. 2009, Reddy and Rao 2002, EPA 2015b).

Carbaryl works by overstimulating the nervous system of target pests (and non-target insects) by facilitating the accumulation of acetylcholine in the neurons. Acetylcholine is an excitatory neurotransmitter that contributes to attention, memory, and involuntary muscle movement in vertebrates and invertebrates (Purves et al. 2001). Carbaryl competitively binds to a serine residue in the active site of acetylcholinesterase (AChE), the enzyme that catalyzes the hydrolysis of acetylcholine to acetate and choline. Binding by carbaryl prevents the breakdown of acetylcholine by AChE (Lee and Barron 2016). With its breakdown blocked, acetylcholine accumulates within the cholinergic synapses of the organism, which leads to neuromuscular paralysis and, eventually, death. While the biological function of the AChE pathway is well-understood in animals, its role in other organisms is not. Horiuchi et al. (2003) reported the presence of the acetylcholine synthesis pathway in plants, fungi, and bacteria, which suggests

that acetylcholine may have an evolutionary history far beyond its function in neurological pathways (Horiuchi et al. 2003, Jeon et al. 2013). Relatedly, sources have reported on the acute and chronic toxicity of carbaryl in cases of extended exposure. The compound is considered toxic, and exposure may lead to severe neurological damage and congenital disabilities when exposure occurs during pregnancy. It is mutagenic and carcinogenic and can lead to kidney, liver, and reproductive damage (Carbaryl 2001) in mammals.

Environmentally, the application of such pesticides raises concerns pertaining to agricultural runoff and subsequent ecological effects. Carbaryl is the second most frequent insecticide found in off-target water sources; the Environmental Protection Agency has detected the compound in up to 50 percent of urban streams (Hoffman et al. 2000). It is toxic to aquatic invertebrates, fish, and other marine and freshwater organisms. As a broad-range insecticide, carbaryl also kills beneficial insects. Thus, its application is not authorized when plants are in bloom to protect bees and other pollinators (EPA 2003). The EPA has documented phytotoxicity following carbaryl application in members of the Vitaceae (i.e., grapevine) family, including Virginia creeper (*Parthenocissus quinquefolia*) and Boston ivy (*Parthenocissus tricuspidata*), but not in *Vitis* species (EPA 2015b). For environmental and human health reasons, the European Commission prohibits the use of carbaryl as a means of plant protection in countries in the European Union. In the United States, however, the use of carbaryl in agriculture is permissible for use according to EPA regulations (EPA 2004), and it remains the third most used insecticide for a variety of purposes, ranging from home garden use to livestock and crop protection in commercial agriculture.



## **Insecticides That Damage Plants**

Commercialized insecticides are thoroughly tested to ensure their application does not harm the plants they are intended to protect. In rare instances, however, certain chemicals cause irreparable plant damage. To my knowledge, only two examples of insecticide-plant interactions have been thoroughly investigated: one in tomato and one in maize. In tomato plants carrying the *Pto* bacterial resistance gene, leaf tissue necrosis has been observed following the application of fenthion, an organophosphate compound (Martin et al. 1994). Martin et al. (1994) determined *Pto* to be a putative serine/threonine protein kinase that confers resistance to *Pseudomonas syringae* pv *tomato*, the pathogen responsible for bacterial speck disease. Leaves of tomato cultivars containing the *Pto* gene product cause fenthion sensitivity, manifested as necrotic leaf lesions.

In maize, physiological damage to the mitochondria was observed in Texas cytoplasmic male-sterile (TMS) cultivars following the application of methomyl, a methyl-carbamate compound marketed as Lannate®. Biochemical impacts include inhibition of malate and pyruvate oxidation and the overstimulation of succinate oxidation, manifesting as decreased mitochondrial matrix density (Koeppel et al. 1978). Despite being categorized as members of different insecticide families (**Figure 1**), carbaryl (Sevin), fenthion, and methomyl (Lannate) possess similar modes of action: they function by inhibition of acetylcholinesterase (Blacker et al. 2010, “Fenthion”, Lin et al. 2020, Moser 2014). In specific circumstances, broad-range insecticides have been reported to have adverse, albeit not lethal, effects on other plant processes, such as effects on yield and disruption of development, metabolism, and photosynthesis (Giménez-Moolhuyzen et al. 2020).

Relatedly, understanding the extent and consequences of insecticide use on plants is critical for minimizing unintended ecological harm while ensuring crop protection and management. Despite efforts to control chemical use, unintended harm to non-target organisms, including beneficial insects and plants, remains a significant concern. Insecticide damage on plants may be more prevalent than previously recognized, indicating potential implications for ecological and agricultural sustainability. Several studies suggest carbamate products may adversely affect root tip growth and respiration (Ennis 1948, Lichtenstein et al. 1962). Shakir et al. (2018) indicated that pesticide treatment may affect shoot tissues more significantly than root tissues; however, an extensive literature search revealed that this phenomenon has not explicitly been evaluated in species treated with carbaryl (Shakir et al. 2018). Here, I present evidence suggesting that carbaryl causes severe damage to the foliage of *Vitis rupestris* B38, a genotype often used for disease-resistance breeding.

In 2019, interveinal necrosis was observed in a hybrid F1 population of seed parent *Vitis rupestris* B-38 and pollen parent *Vitis riparia* HP1 in Geneva, New York. Initially, the necrosis was presumed to result from nutrient deficiency, as similar symptoms have been observed in cases of severe phosphorus or magnesium deficiency (Ashley 2009). Upon further evaluation, the necrotic phenotype appeared to follow the application of carbaryl. The progeny of this interspecific cross, replicated in Springfield, Missouri, were subsequently treated with carbaryl, producing necrotic symptoms in the leaves indistinguishable from those observed in New York. In both locations, carbaryl treatment followed the standard protocol recommended by the manufacturer (Bayer CropScience, St. Louis, MO USA) (EPA 2015b). Through field observations, *in vitro* experimentation, and molecular analysis, I evaluate the role of carbaryl

treatment in the observed interveinal necrosis phenotype in *V. rupestris* hybrids and explore the effects of the phenotype on a genomic level.

## METHODS

### Plant Material

The F1 progeny used in this study resulted from an interspecific cross between seed parent *V. rupestris* B-38 (GRIN ID PI588160) and pollen parent *V. riparia* HP1 (GRIN ID PI588271). The cross was made by Jason Londo in 2014 at the Agricultural Research Station in Geneva, New York (henceforth referred to as NY). The progeny, named JL14\_160×271, were planted in Geneva and vegetatively propagated to establish a replica planting in 2018 at the Darr Agricultural Research Center in Springfield, Missouri (henceforth referred to as MO). The row and vine spacing in NY was 6 feet and 18 feet, respectively, with north-to-south row orientation. The replica vineyard in MO was planted with 0.914 m vine and 1 m row spacing. Row orientation was north-to-south.

### Phenotyping in NY and MO Vineyards

Following observations of interveinal leaf tissue necrosis in the NY vineyard, the MO population was treated with carbaryl using the commercial product Sevin SL (Bayer). At both locations, the insecticide was applied at 814 mL of active ingredient per acre, which is the concentration recommended by the supplier. In NY, Sevin SL was applied using a mechanized sprayer; in MO, it was applied using a SOLO 425 backpack sprayer. In MO, Sevin SL was applied as a 0.0106% suspension. Individual vines were scored for the presence (score of 1,

sensitive vines) or absence (score of 0, insensitive vines) of leaf necrosis one week following carbaryl application at the NY site (n = 222) and the MO site (n = 290) in 2020.

### ***In Vitro* Leaf Disk Bioassay**

In 2021, an *in vitro* bioassay was conducted using leaf disks to assess the variability of the interveinal necrosis phenotype in response to carbaryl under controlled environmental conditions. Leaves of 259 hybrid and seven parental genotypes (six *V. rupestris* seed parents and one *V. riparia* pollen parent) were collected from the MO vineyard. Vines to be tested were chosen based on their viability in the field. The third and fourth leaves were collected from each individual, counting from the shoot tip. Leaves were placed in a plastic bag, labeled with the corresponding vine identification number, transported to the lab where they were sterilized in 10% Clorox® for 10 minutes, and rinsed for three minutes in three consecutive baths of fresh deionized water. Following sterilization, leaves were blotted dry between sterilized paper towels. A total of eight leaf disks were cut from each genotype. Four leaf disks for the control group were dipped in a solution containing 2 µL of Tween 20 to decrease water surface tension and 100 mL of sterile deionized water and plated on a 1% water agar plate. The remaining four disks were dipped in a suspension containing 100 mL of sterile deionized water, 2 µL of Tween 20, and 530 µL of Sevin SL (0.53% concentration, which corresponds to 50x the recommended field concentration) and plated on a 1% water agar plate. Each leaf disk was plated with the abaxial side up. The agar plates for both the control and treated leaf disks were placed in a plastic bag and incubated in a growth chamber for three days at 21°C under a 15-hour light/9-hour dark cycle.

## Scoring of *In Vitro* Leaf Disks

After three days of incubation, each genotype was scored individually by two people to account for bias. Each disk was scored for the severity of necrosis on a scale of one to nine. A score of one indicated no change in the leaf disk (compared with the control agar plate for the same individual). A score of two signified discoloration of the leaf disk but no necrosis. A score of three indicated the presence of necrosis that covered less than fifty percent of the disk. A score of four approximated fifty percent coverage of necrosis on the leaf disk; five indicated that slightly more than fifty percent of the leaf disk was affected. A score of six signified that between fifty and seventy-five percent of the disk was affected. A score of seven signified that more than seventy-five percent of the leaf surface was affected by necrosis, with the perimeter of the disk left unaffected. Eight indicated necrosis on nearly the entire leaf disk, including the perimeter. A score of nine signified complete necrosis of the leaf disk (**Table 2; Figure 2**). The scores from each person for each genotype were averaged to create a single score for the control and a single score for the carbaryl-treated leaf disks for each genotype.

## QTL Mapping

Quantitative trait locus (QTL) mapping was performed in the statistical software R version 3.6.3 (2020-02-29) using the *qtl* package (Broman et al. 2003). Linkage to the sensitivity phenotype was established using composite interval mapping (Jansen and Stam 1994, Zeng 1994) separately in the female and the male genomes to improve the precision of QTL detection. Logarithm of odds (LOD) significance threshold values at alpha of 0.05 and 0.01 were established using a 1000-fold permutation test. LOD values were calculated using the *traitCIM* function and histograms were plotted using MapChart (Voorrips 2002). Only LODs that

exceeded the significance threshold at  $p < 0.05$  were considered significant. The percentage of variance explained was calculated using *fitqtl* via the Haley-Knot regression method (Haley and Knott 1992).

### **RNA Extraction and RNA-seq Analysis**

Thirty-two vines grown at the MO site were selected for gene expression analysis. Sixteen of them were selected on the basis of scoring as insensitive (IN), and an additional sixteen as sensitive (SE) with consistently severe necrotic symptoms. The selected vines were sprayed with 50x the recommended field concentration (0.53% Sevin SL) to accelerate the development of the necrotic phenotype. Leaf tissue was collected in bulk for SE and IN groups (i.e., groups of individuals with similar phenotypes but different genotypes) at the following time points: before exposure (0 hours), 24 hours following carbaryl exposure, 48 hours following carbaryl exposure, and 72 hours following carbaryl exposure. Collected tissues were immediately flash-frozen in liquid nitrogen and stored at  $-80^{\circ}\text{C}$  until RNA extraction. Before extraction, leaf tissues for each phenotype were ground under liquid nitrogen. Immediately following grinding, extraction was performed using the Spectrum Plant Total RNA Kit (protocol B), with the addition of PVP-40 to the lysis buffer (3.6%), as performed by Gambino et al. (Gambino et al. 2008). All centrifugation steps were carried out at  $4^{\circ}\text{C}$ . RNA was quantified using the Qubit fluorometry and RNA Quantification Kit. RNA was stored at  $-80^{\circ}\text{C}$  until amplification and sequencing. Library construction and sequencing were performed at the Genome Sequencing Facility of the University of Kansas Medical Center. Sequencing libraries were constructed using the TruSeq Stranded mRNA Sample Preparation Kit by Illumina Corporation (San Diego, California, USA). The unique dual-indexed libraries were amplified,

quality-checked and paired-end sequenced at 150-bp read length on two flow cells in a NovaSeq 600 instrument.

RNA-seq data were analyzed for differential gene expression using the bioinformatics software CLC Genomics Workbench v20.0.4 (Qiagen Bioinformatics, Redwood City, California, USA). RNA-seq analysis was conducted on SE and IN plants in three technical replicates. Samples were imported as paired reads and filtered based on length (between 15 and 1000 nt) and quality (limit 0.05) using the software's default parameters. Reads were mapped to the *Vitis vinifera* 12x reference genome sequence (Canaguier et al. 2017) downloaded from the ENSEMBL database using default parameters. Expression data were normalized from mapped reads as the number of reads per kilobase per million reads mapped (RPKM). To identify genes that were differentially expressed between SE and IN plants, genes with 4-fold higher or 4-fold lower RPKM values (at FDR-adjusted  $p \leq 0.01$ ) across SE and IN plants were filtered. This process was performed for the 24-, 48-, and 72-hpt time points. In total, 238 genes were identified as differentially expressed between IN and SE plants. For each read, probable protein functions were identified via the Gramene Genome Browser (Ware 2007) and the Basic Local Alignment Search Tool (BLAST) (Mount 2007).

### **Validation of RNA-seq Results Using RT-qPCR**

To validate RNA-seq data, three SE plants (16, 49, and 69) and three IN plants (112, 183, and 222) were grown and carbaryl-treated by a spray application of a 0.53% Sevin SL solution in the greenhouse (**Table 3, Figure 3**). Total RNA was extracted from leaves collected from three individuals of each genotype at each time point (0-, 24-, 48-hpt). The RNA was then reverse transcribed from random hexamers using SuperScript IV® First Strand cDNA synthesis Kit

Reverse Transcriptase (Invitrogen) and Oligo(dT), according to the manufacturer's recommendations.

Primers for *Actin3* (reference), *EDS1*, and *NDR1-HIN1* genes were designed using the *V. vinifera* reference genome and GenBank Primer-BLAST. The concentration of cDNA samples was adjusted based on cycle threshold ( $C_t$ ) values obtained from real-time qPCR (RT-qPCR) runs with *Actin3* primers. A standard curve was constructed for each transcript using the PCR product generated for each primer pair. Single reactions were prepared in technical triplicate using the PowerSYBR® Green Master Mix from Thermo Fisher Scientific. RT-qPCR reactions for each primer pair were performed alongside an *Actin3* control to assess the efficiency of the reaction and a non-template negative control to check for contamination. Each reaction (20  $\mu$ L total volume) contained 2  $\mu$ L of diluted cDNA and 0.5  $\mu$ L each of forward and reverse primer. The RT-qPCR was run using the QuantStudio 6 Pro real-time PCR system from Thermo Fisher Scientific. The cycling conditions were one cycle of denaturation at 95°C/10 min, followed by 40 three-segment cycles of amplification (95°C/15 sec, 57°C/30 sec, 72°C/40 sec) and one three-segment melting cycle (95°C/15 sec, 60°C/1 min, 95°C/1 sec (dissociation)). The baseline adjustment method of the QuantStudio 6 Pro software was used to determine the  $C_t$  for each reaction. All samples were amplified in triplicate, and the mean was used for further analyses.

## RESULTS

### Symptoms and Segregation of Interveinal Necrosis in NY and MO

Following a Sevin SL insecticide spray application, necrotic symptoms were observed on the leaves of a subset of the JL14\_160×271 hybrid grape progeny at the NY site. Approximately half of the vines developed necrotic lesions, while others remained symptomless. The condition



appeared more severe in fully expanded leaves and resembled symptoms of phosphorus or magnesium deficiencies. The necrotic lesions spread into the leaf blade's interveinal areas, avoiding petiolar, proximal, distal, and mid veins. Areas surrounding the major veins remained green even when interveinal tissues died. Symptoms did not coincide with regions of the leaf which were in direct contact with carbaryl; instead, necrosis appeared to spread systemically in a characteristic interveinal pattern and affected either the entire or a section of the leaf blade (**Figure 4**). Necrosis also developed on leaves of the seed parent *V. rupestris* B-38, but not on the pollen parent. Field phenotyping of interveinal necrosis in the NY and MO vineyards revealed that cohorts of SE and IN plants partially overlapped at the two locations. In NY, 51% of individuals displayed symptoms of interveinal necrosis. In contrast, in MO, 69% displayed symptoms of interveinal necrosis (**Figure 5**). A comparison of the NY and MO phenotype data revealed that 70% of individual vines that were present in both locations were concordant in their symptom development (presence or absence of necrosis) across the NY and MO locations.

### **QTL Mapping Based on NY and MO Field Data**

The 70% concordance in the carbaryl-triggered symptom between the NY and MO locations suggested that carbaryl-sensitivity may have a genetic component. To test this hypothesis, QTL mapping was performed to detect if a locus in the genome is linked to this phenotype. A linkage map constructed for the parents of this F1 progeny (Bhattarai et al. 2021) and the high heterozygosity of grapevine enabled the mapping of carbaryl sensitivity to a locus of the grape genome. Mapping of the carbaryl sensitivity data collected in the NY vineyard during the 2020 field season yielded two QTL peaks which crossed the LOD significance threshold at an alpha of 0.05 based on a 1,000-fold permutation test. One mapped to

chromosome 16 of the seed parent's genome between markers 16\_2848590 and 16\_15267213 with 99% confidence and explained 20.42% of the phenotypic variance. This QTL encompasses a region of approximately 11.0 centimorgans. The other significant QTL was identified on chromosome 10 between markers 10\_1472990 and 10\_3457871 with 95% confidence (**Figure 6A, B, and F**). Mapping the QTL to the seed parent genome agreed with our observation that the seed parent, but not the pollen parent, was sensitive to carbaryl.

QTL mapping of the carbaryl sensitivity data collected in the MO vineyard in 2020 was based on the presence or absence of interveinal necrosis. Carbaryl sensitivity was mapped to a single locus on chromosome 16 in the female parent between markers 16\_2848590 and 16\_12991399 (**Figure 6C, D, and G**). This locus overlaps the same genomic region that was identified via QTL mapping performed using data collected from NY. The QTL was mapped with 95% confidence and explained 16.82% of the variance. Mapping the MO data, however, did not reveal any other QTL in the genome. **Figures 6F, 6G and Figure 7C** delineate the region under the peak on chromosome 16 as it aligns with the *V. vinifera* reference genome (Canaguier et al. 2017).

### **QTL Mapping Based on the *In Vitro* Leaf Disk Bioassay**

To confirm QTL mapping results obtained on the basis of field phenotypes, I performed an *in vitro* leaf disk bioassay to generate phenotype data under precisely controlled environmental conditions. The leaf disks analyzed in the bioassay also produced necrosis, but the shape of necrotic spots did not have recognizable patterning. In SE leaf disks, necrotic lesions developed within 72-hpt (**Figure 2**). The average scores minus the control scores mapped between markers 16\_7987237 and 16\_15792111 with 95% confidence and explained 30.33% of

the phenotypic variance. This QTL encompasses a region of approximately 9.0 centimorgans (**Figure 7**). The average scores and the individual scores were also mapped between markers 16\_7987237 and 16\_15792111 (**data not shown**). The individual leaf disks of the seed parent (*V. rupestris*) consistently scored 8 (**Table 2**) or greater, while the individual leaf disks of the pollen parent consistently scored 2 or less. The frequency of phenotype scores across individuals was continuous (**Figure 8**).

### **Gene Content of the QTL Region**

As I did not have access to the genome sequence of the female parent, I examined the gene content corresponding to the region located under the QTL peak in the *Vitis vinifera* reference genome sequence (RefSeq genome). This region encompasses 196 genes. Of these, 33 genes are involved in perception and response to environmental cues. These include 11 receptor-like kinases, 15 ethylene-responsive transcription factors (ERFs), six nucleotide-binding site leucine-rich repeat (NBS-LRR) proteins, and one ABA-responsive transcription factor (AREB proteins). NBS-LRR proteins are well-known for their role in pathogen detection (Jones et al. 2016, Stroud et al. 2022). ERFs are also known to cross-talk with the jasmonic acid-signaling pathway to activate defense responses (Lorenzo et al. 2003).

### **RNA-seq Analysis in Carbaryl-Treated Sensitive and Insensitive Plants**

To gain insight into the impact of carbaryl on the grape leaf transcriptome, a comparative RNA-seq analysis was conducted on treated F1 hybrids. A summary of the sequencing and read-mapping data is shown in **Table 4**. A gene was considered up- or down-regulated if its transcript abundance changed at least two-fold up or down at  $p \leq 0.05$  at any of the three time points

following carbaryl treatment. This screening led to the identification of between 3,043 and 5,432 differentially expressed genes (DEGs) at each time point in SE plants (**Table 5**). To obtain a smaller subset of genes, a more stringent filtering was performed, in which a gene was considered up- or down-regulated if its transcript abundance changed at least four-fold up or down (**Table 5, Figure 9**) at any of the three time points following carbaryl treatment. This screening led to the identification of between 460 and 1,090 DEGs. A p-value of  $\leq 0.01$  was used to identify a total of 238 DEGs (**Figure 10**) for further analyses.

Lists of differentially regulated genes were subjected to gene ontology (GO) enrichment analysis, the results of which pointed to the activation of several biological functions that are characteristic of pathogen-triggered salicylic acid-mediated defense response. These included the upregulation of shikimic acid pathway, calcium-mediated signaling, chitin catabolism, defense against hydrogen peroxide, phenylpropanoid biosynthesis and cell wall organization and biogenesis (**Figure 11**). Additional biological processes also activated, but not directly related to defense included abscisic acid and ethylene signaling pathways, nitrogen compound detoxification, toxin catalytic processes, cytokinin metabolism, auxin response, phloem development and mitotic cell cycle transition (**Figure 11**). Overall, defense-related biological processes appeared to have the most prominent part in the carbaryl-triggered response.

In addition to GO enrichment data, two other observations pointed to the key role played by a defense-like mechanism. Firstly, *EDSI*, a biomarker and key regulator of both salicylic acid (SA)- and jasmonic acid (JA)-mediated defense pathways reached several-fold higher expression in SE than in IN plants. Secondly, the minor QTL that was detected in NY, though not in MO, coincided with the downy mildew resistance locus mapped previously by Bhattari et al (2021). After having carefully scanned all defense- and stress-related structural and regulatory DEGs, I

selected those that specifically responded to carbaryl in SE plants, but not in IN plants, and focused my further analysis on this subset of genes.

### **Defense Genes of Interest Identified by RNA-seq Analysis**

The transcription of *enhanced disease susceptibility 1 (EDSI)* and *senescence-associated gene 101 (SAG101)* occurred at a constitutively higher level in the SE, but not in the IN plants. The protein products of *EDSI* and *SAG101* associate with one another and act as master regulators of the SA-mediated pathogen defense pathway (Tan et al. 2015). Both genes displayed greater upregulation in the SE plants compared with the IN plants at 24-, 48-, and 72-hpt (**Figure 12**). The greatest change in *EDSI* and *SAG101* transcription occurred between 0- to 24-hpt, during which *EDSI* was 2.72-fold and *SAG101* was 2.47-fold upregulated in SE plants. During the following 48-hour time period, the transcription of both *EDSI* and *SAG101* remained stable in the SE plants. In the IN plants, the most significant change in expression occurred between 48- and 72-hpt, at which time *EDSI* was 5.15-fold, and *SAG101* was 2.35-fold down-regulated.

Additional genes associated with SA-mediated signaling were also expressed at a constitutively higher level following carbaryl treatment. Transcripts of these genes increased gradually but steadily, reaching their maximum level only at 72-hpt. In the IN plants, many of the same genes did not change their expression level relative to the control during the 72 hours of the study. Examples of these genes are *stilbene synthase 2* and *trans-resveratrol di-O-methyltransferase* (**Figure 13**), *NDR1/HIN1-like protein 6 (NHL6)* (**Figure 14**), *dirigent protein 22*, *heat stress transcription factor B-3*, *PR-10* and *PR-1*, and *AAA-ATPase ASD* (**Table 6**). Other SA-responsive genes showed a temporary up-regulation at 24-hpt in IN plants, followed by a return to control levels by 48- and 72-hpt. In SE plants, these genes gradually but steadily

approached their highest levels of expression by 72-hpt. Examples of such genes include several *MYB* and *WRKY* transcription factors, *cytochrome P450*, *shikimate dehydrogenase*, *cytokinin dehydrogenase*, and *pectinesterase* (**Table 6**).

The expression of *stilbene synthase 2* and *trans-resveratrol di-methyltransferase* (**Figure 13**) steadily increased during the 0-to-72 h period and reached 31.9-fold and 14.9-fold up-regulation, respectively, by 72-hpt in SE plants. *Stilbene synthase 2* and *trans-resveratrol* encode enzymes responsible for the synthesis of trans-resveratrol and pterostilbene, respectively, in grapevine (Pezet et al. 2004, Rukavtsova et al. 2022). Both compounds, members of the secondary metabolite family of stilbenes, are considered phytoalexins that are synthesized in response to pathogen infection (Hasan and Bae 2017). As products of the phenylpropanoid pathway, they are derived from chorismate via phenylalanine.

*NDR1/HIN1-like protein 6 (NHL6)* (**Figure 14**) expression remains comparable in SE and IN plants at 24- and 48-hpt relative to 0-hpt. At 72-hpt, on the other hand, *NHL6* in SE plants reach a level of expression that is 5.5-fold higher relative to 0-hpt while its expression remained at control level in IN plants. The *NDR1/HIN1* gene family is often associated with innate immunity and defense against bacterial and fungal pathogens. The *NHL6* gene has been shown to play a role in coordinating the SA-, JA-, and ethylene (ETH)-related defense signaling pathways (Liu et al. 2020, Yamazaki et al. 2022).

Interestingly, genes characteristically associated with JA-mediated defense regulation also responded to carbaryl treatment. The expression of two such genes, *Jasmonate-induced oxygenase 1 (JOX)* and *ethylene-response factor C3 (ERF.C.3)* (**Figure 15**), followed a pattern characterized by a gradual and steady up-regulation in SE plants and a temporary increase at 24-

hpt followed by control-level expression at 48- and 72-hpt. In IN plants, their expression returned to control levels at 48- and 72-hpt.

### **Validation Using RT-qPCR**

To validate the results of the RNA-seq analysis, three IN and three SE vines (**Table 3**) were rooted and grown in the greenhouse, sprayed with carbaryl as for the RNA-seq experiment, and RNA was extracted from leaves at 0- (control), 24-, 48-, and 72-hpt. All three SE plants developed characteristic leaf necrosis symptoms, while IN plants remained symptomless (**Figure 3**). I attempted to measure the expression levels of the *EDSI* gene, as it is a key regulator of SA-mediated defense, but unfortunately, *EDSI* expression was below the detection level of RT-qPCR (**data not shown**). Therefore, I focused my efforts on another defense response regulator, *NHL6*, the expression of which could be measured in all plants at all time points. The RT-qPCR-measured expression of *NHL6* was indistinguishable in SE and IN plants at all timepoints (**Figure 16**), which meant that these results were inconsistent with the results of the RNA-seq analysis. Taken together, the development of leaf necrosis, and the absence of detectable upregulation of *NHL6* suggest that under greenhouse conditions, carbaryl-induced leaf necrosis is independent from the activation of the defense response.

## **DISCUSSION**

### **Evidence of Insecticide Sensitivity in Grapevine**

I have produced incontrovertible evidence that the insecticide carbaryl causes damage to *V. rupestris* B38, a grape genotype frequently used as a source of disease resistance. To my knowledge, this is only the third known example of an insecticide severely damaging a crop for

which it is labeled. Investigation of the interveinal necrosis phenotype in MO and NY vineyards revealed an approximate 1:1 segregation of carbaryl-sensitivity in an F1 hybrid progeny of *V. rupestris* B38. QTL analysis showed that carbaryl sensitivity was linked to a region on a chromosome 16 haplotype of the female parent. Regardless of whether phenotype data were collected in the field or *in vitro*, and whether the field data originated from NY or MO, a major QTL for this trait was mapped to the same locus in the female genome (**Figures 6 and 7**). The carbaryl sensitivity trait appears quantitative, as demonstrated by the relative low percent of variance explained by the locus, the imperfect concordance of SE F1 individuals observed in NY and MO (**Figure 5**), the variation in the extent of the QTL interval (**Figures 6 and 7**), and the broad distribution of symptom intensity in SE plants *in vitro* (**Figure 8**). The imperfect concordance of symptoms across NY and MO locations suggests that the environment influences the severity of the necrotic response. It is also likely that differences in phenotypes across locations are due to variability in phenotypic scoring, as phenotyping was conducted by different individuals at each location (**Figure 5**).

### **RNA-seq Analysis in Carbaryl-Treated Sensitive and Insensitive Plants**

In the *Vitis vinifera* RefSeq genome, the region corresponding to the QTL contains 33 genes that are involved in perception and response to environmental cues. To explore the possibility that some of these respond to carbaryl, and to gain insight into the molecular mechanisms underlying interveinal leaf necrosis, an RNA-seq analysis was performed at three time points (24-, 48-, and 72-hours) following carbaryl application under field conditions in MO. These findings revealed a consistent upregulation of numerous genes involved in plant pathogen defense pathways, particularly within the SA-mediated pathway which produces hypersensitive



response (HR) (**Table 6**). HR involves active cell death (apoptosis) which produces necrotic lesions of varying severity. The carbaryl-triggered interveinal necrosis symptoms observed in *V. rupestris* B-38 and in its SE F1 progeny also appeared to be the result of an HR-like apoptotic event. Furthermore, the heightened expression of defense-related genes observed specifically in the SE plants suggested that defense-mechanisms may be activated by carbaryl application. The presence of *receptor-like kinase* and *NBS-LRR* genes in the QTL region contributed to the proposed defense-response hypothesis. The protein products of such genes are known to function as receptors for pathogen-associated molecular patterns or sentinels for pathogen effector activity (Zhou and Zhang 2020). Even though none of these genes had a dramatic transcriptional upregulation, their protein products may have played a critical part in the apoptotic response to carbaryl. Therefore, I decided to explore genes that were upregulated in SE plants, but not in IN plants, and were explicitly known to be part of plant defense. It is important to note, however, that upregulation of numerous defense-related genes can occur not only in response to pathogen attack but to various other forms of environmental stress, including dramatic change in temperature, drought, or wounding (Morel and Dangl 1997). It is equally important to consider that genes unrelated, or not directly related, to defense were also activated, leaving open the possibility that the apoptotic response was set into motion by abscisic acid, ETH signaling or detoxification pathways (**Figure 11**).

### ***EDS1 and SAG101***

Findings from previous studies indicate that in wild-type plants, pathogen infection specifically triggers the activation of SA- and JA-related genes (summarized in **Table 6**). To gain insight into transcriptional changes associated with the early development of carbaryl-triggered

leaf necrosis, the regulation of such genes was closely investigated. Arguably, the most revealing transcriptional change detected in SE plants was the significant and stable up-regulation of the *EDS1* and *SAG101* genes (**Figure 12**), the protein products of which form a principal regulatory node in the SA-mediated immune response. EDS1 is a key regulator for biotrophic pathogen resistance, and its expression is considered a biomarker for effector-triggered immunity (ETI). The protein plays a central role in orchestrating defense responses within SA-mediated pathways and is commonly triggered upon exposure to pathogens (Gao et al. 2010). Its regulatory role extends to the initiation of HR and the priming of unaffected tissues for impending pathogen attack, a phenomenon termed systemic acquired resistance (Gao et al. 2010). Congruent with EDS1, SAG101 contributes to SA accumulation and is also considered a central component of plant pathogen resistance (Lu 2009, Wang et al. 2020). EDS1 has been shown to interact with SAG101, and the EDS1/SAG101 complex is at the receiving end of signals transduced by NBS-LRR and receptor-like kinases (Chen et al. 2022). While the intricate details of the EDS1/SAG101 complex are still under investigation, RNA-seq results (**Figure 12**) raised the possibility that components of the *V. rupestris* B38 defense system may identify carbaryl as a xenobiotic threat.

### ***NHL* Genes and Salicylic Acid Biosynthesis**

The family of genes encompassing several NDR1/HIN1-like protein complexes has also been shown to play a role in early plant pathogen defense in response to biotrophic pathogens (Liu et al. 2020). *Nonrace-specific disease resistance gene 1* (*NDR1*) and *Harpin-induced gene 1* (*HIN1*) (collectively referred to here as *NHL* genes) show high sequence similarity across organisms and play a vital role in plant disease resistance, including reported involvement in HR

and leaf senescence. Additionally, *NHL* genes are essential in abiotic stress responses such as extreme temperature, salinity, and drought (Guo et al. 2023). Chong et al (2008) indicate that orthologs of *Arabidopsis NDR1* and *EDSI* in *V. vinifera* influence genomic interactions in SA- and JA/ETH-mediated pathways (Chong et al. 2008). Although additional experimentation is required to validate these results, RNA-seq analysis (**Figure 14**) appears consistent with the literature, further suggesting the defense-related response to carbaryl in SE plants.

Though the details of SA biosynthesis are still not fully understood, it is widely accepted that two possible pathways can synthesize SA: the phenylalanine ammonia-lyase (PAL) pathway and the isochorismate synthase (ICS) pathway, the latter of which is apparently upregulated upon carbaryl exposure. ICS involves the conversion of chorismate to isochorismate, which is subsequently converted into SA. Chorismate originates from the shikimate pathway, which is alternatively responsible for the production of secondary metabolites and aromatic amino acids (Lefevre et al. 2020). The shikimate pathway is also commonly known as the starting point for resveratrol (stilbene) synthesis (Averesch and Krömer 2018, Jones et al. 2016). Stilbenes and resveratrol are secondary metabolites which are known to act as phytoalexins to the downy mildew and the powdery mildew pathogens in grapevine. According to the RNA-seq results, *stilbene synthase 2* and *trans-resveratrol di-O-methyltransferase* (**Figure 13**) are expressed at a higher level at 72 hours in SE plants compared with the highest level of expression in IN plants (24 hours).

Relatedly, an HR has been identified by Chang et al. (2011) in *V. rupestris* in response to the *Erwinia amylovora*-secreted effector Harpin. The activation of Harpin led to heightened expression of stilbene synthase genes, resulting substantial accumulation of trans-resveratrol, thereby boosting resistance against disease. Chang et al. (2011) compared Harpin-induced trans-

resveratrol accumulation in pathogen-resistant *V. rupestris* to that in the pathogen-sensitive *V. vinifera* ‘Pinot Noir’ cultivar. They observed that the accumulation of trans-resveratrol as early as 10 hours post-Harpin exposure, followed by a return to post-exposure levels by 48 hours was conducive to a successful HR in *V. rupestris* (Chang et al. 2011). Interestingly, the pattern of Harpin-triggered *trans-resveratrol* expression reported by Chang et al. (2011) is similar to the carbaryl-induced *trans-resveratrol* expression observed in IN plants in the presented RNA-seq results (**Figure 13**).

Harpin-induced genes (*HINI*), broadly categorized as NHL genes, are known for triggering plant immune defense in response to pathogens. Harpin proteins produced and released by pathogens upon infection may activate NHL genes, indicating that the upregulation of *NHL6* (**Figure 14**) may contribute to a reaction that is similar to Harpin-induced HR (Bao et al. 2016).

### ***WRKY* Transcription Factors, *JOX*, and *ERF.C.3***

Members of another family of regulators that were activated by carbaryl exposure are the WRKY transcription factors. *WRKY75* is activated in response to carbaryl in both IN and SE plants, with a delayed upregulation in SE plants (**results not shown**). In *Arabidopsis*, members of the WRKY family are involved in SA-mediated signaling (Lu 2009) and in regulating ICS activity (van Verk et al. 2011, Wang et al. 2014). *WRKY75* (**Table 6**) is involved in the ICS pathway, leaf senescence (Chen et al. 2021), and lateral root development (Rosado et al. 2022). It has been demonstrated in several plant species that WRKY transcription factors are positive regulators of JA- and ETH-mediated plant pathogen defense, which are also commonly activated in plants in response to necrotrophic pathogens and abiotic stressors. In *Arabidopsis*, *WRKY75*

regulates the expression of *jasmonate-induced oxidase (JOX)* and *ethylene response factor C3 (ERF.C.3)* genes in the JA pathway (Chen et al. 2021). Importantly, the increase in *WRKY75* expression (**Table 6**) was paralleled by an up-regulation of both *JOX* and *ERF.C.3* in carbaryl-treated grapevine leaves (**Figure 15**). It is also interesting that the expression pattern of *JOX* and *ERF.C.3* are different in SE and IN plants: the transcription of both genes were sharply upregulated at 24-hpt then dropped back to control level in IN plants, whereas their transcription gradually increased through the 0- to 72-hpt time frame in SE plants (**Figure 15**). Additionally, WRKY factors are regulators of pathogenesis-related (PR) proteins which is a collective category of many diverse proteins, including chitinases, which contribute to fungal pathogen defense (Heil and Bostock 2002), and allergens, which function in several categories of plant stress defense (Sinha et al. 2014). RNA-seq analysis revealed similar patterns of upregulation in these factors in response to carbaryl application: *PR-10*, *PR-1*, and *chitinase* (**Table 6**) are expressed at substantially higher levels at 72 hours in SE plants compared to any time point in IN plants (**results not shown**).

### **Cross-Talk Between Salicylic Acid- and Jasmonic Acid-Mediated Pathways**

Considered collectively, RNA-seq results imply that SE plants respond to carbaryl exposure by activating various defense-related pathways, including those mediated by SA, JA, ETH, and potentially abscisic acid signaling (summarized in **Table 6** and **Figure 11**). Previous studies suggested that in wild-type plants, these pathways may interact synergistically or antagonistically depending on the type of stress experienced by the plant (Stroud et al. 2022). RNA-seq results highlight a number of gene expression changes that are indicative of communication between the SA and JA defense pathways, commonly referred to as “cross-talk”

(Stroud et al. 2022). Steady upregulation of *EDSI* and *SAG101* implies an SA-dependent defense response, while activation *JOX* and *ERF* indicate a JA-dependent response. The possibility of a cross-talk between JA and SA signaling is strengthened by expression of *WRKY75*. Several other WRKY transcription factors also act as signal integrators for the two pathways (Li et al. 2017). Additionally, *nonexpressor of pathogenesis-related genes (NPR1)* interact with transcription factors of both pathways to modulate defense response (Spoel et al. 2003). It is well established that pathogen infection triggers the activation of SA- and/or JA-related regulators, but I have yet to reach a complete understanding of how these pathways interact to execute a defense strategy (Stroud et al. 2022) in response to carbaryl.

Taken together, the carbaryl-induced gene expression pattern in SE plants points to a hypothesis that carbaryl triggers a complex defense response which culminates in robust HR and leads to the apoptosis of large sections of the leaf blade. However, the results of my RT-qPCR gene expression study, in which I repeated the carbaryl treatment experiment on greenhouse-grown plants, disagreed with the RNA-seq results. In the greenhouse experiment, the expression of the *NHL6* gene was indistinguishable in SE and IN plants. Nonetheless, SE plants developed the characteristic leaf necrosis symptoms, and IN plants remained symptomless. Considering that my carbaryl-triggered defense hypothesis rested on the differential expression of such essential defense-regulated genes as *NHL6* in SE, the greenhouse results are inconsistent with my hypothesis and suggested that there might be an entirely different mechanism that leads to leaf necrosis.

The possibility cannot be excluded, however, that the inconsistent *NHL6* expression pattern was due to the young age of the plants and conditions under which they were grown in the greenhouse. The greenhouse plants used for the RT-qPCR experiment were four months old

and were propagated from dormant cuttings. In contrast, the plants used in RNA-seq analysis were well established 4-year-old vines grown in the field. Propagation from dormant cuttings involves rooting, which requires the incubation of a one-year-old dormant stem sections with a fresh cut in moist growth medium for several weeks. Under these conditions, infection by opportunistic pathogens through the open xylem vessels are possible and the resulting endophytic growth of such organisms may lead to the maintenance of a defense state even after the plants have rooted. Additional conditions that differed between the two experiments were the artificial versus natural light under which the plants were grown, the presence versus absence of fertilization and the artificially inoculated versus natural root microbiome.

Therefore, before rejecting the carbaryl-triggered defense hypothesis, it is important to repeat the experiment under conditions that are identical or closer to the field conditions. Additional pharmacological experiments could also offer insight into the role plant hormones play in the necrotic response. For instance, hormones such as methyl salicylate, methyl jasmonate, or ETH could be tested if they in themselves produce necrotic symptoms, or if they exacerbate, mitigate or block the carbaryl-induced reaction. Furthermore, examining the carbaryl response in plants exposed to environmental stressors such as drought, salinity, or extreme temperatures may also shed light on the mechanisms underlying carbaryl-triggered necrosis.

In summary, I provided evidence that the insecticide carbaryl is the causative agent of interveinal leaf necrosis in *V. rupestris* B38 its progeny that inherited the 15- to 24-cM region of one of its chromosome 16 haplotypes. Though my studies of the underlying mechanisms produced inconclusive results, they did point to future experiments that will potentially illuminate the molecular basis of this interaction.

## REFERENCES

- Ashley R. 2009. Grapevine Nutrition- An Australian Perspective.
- Atwood D, Paisley-Jones C. 2017. Pesticides industry sales and usage: 2008–2012 market estimates. US Environmental Protection Agency, Washington, DC.
- Averesch NJH, Krömer JO. 2018. Metabolic Engineering of the Shikimate Pathway for Production of Aromatics and Derived Compounds-Present and Future Strain Construction Strategies. *Front Bioeng Biotechnol* 6:32.
- Babinska I, Banaszkiwicz T, Baran MP, Zakrzewska M. 2010. Influence of pesticide dump on the environment. Department of Land Reclamation and Environmental Management, University of Warmia and Mazury in Olsztyn.
- Bao Y, Song W-M, Pan J, Jiang C-M, Srivastava R, Li B, Zhu L-Y, Su H-Y, Gao X-S, Liu H, et al. 2016. Overexpression of the NDR1/HIN1-Like Gene NHL6 Modifies Seed Germination in Response to Abscisic Acid and Abiotic Stresses in Arabidopsis. *PLoS One* 11:e0148572.
- Benheim D, Rochfort S, Robertson E, Potter ID, Powell KS. 2012. Grape phylloxera (*Daktulosphaira vitifoliae*) - a review of potential detection and alternative management options. *Ann Appl Biol* 161:91–115.
- Bhattarai G, Fennell A, Londo JP, Coleman C, Kovacs LG. 2021. A Novel Grape Downy Mildew Resistance Locus from *Vitis rupestris*. *Am J Enol Vitic* 72:12–20.
- Blacker AM, Lunchick C, Lasserre-Bigot D, Payraudeau V, Krolski ME. 2010. Toxicological Profile of Carbaryl. *In* Hayes' Handbook of Pesticide Toxicology. pp. 1607–1617. Elsevier.



- Broman KW, Wu H, Sen S, Churchill GA. 2003. R/qtl: QTL mapping in experimental crosses. *Bioinformatics* 19:889–890.
- Bond C, Cross A, Buhl K, Stone D. 2016. Carbaryl General Fact Sheet. National Pesticide Information Center, Oregon State University Extension Services. as found on the website (<http://npic.orst.edu/factsheets/carbarylgen.html>). Accessed 28 November 2023.
- Canaguier A, Grimplet J, Di Gaspero G, Scalabrin S, Duchêne E, Choisine N, Mohellibi N, Guichard C, Rombauts S, Le Clainche I, et al. 2017. A new version of the grapevine reference genome assembly (12X.v2) and of its annotation (VCost.v3). *Genom Data* 14:56–62.
- Carbaryl. 1994. No. 153. World Health Organization.
- Carbaryl. 2001. Beyond Pesticides. as found on the website (<https://www.beyondpesticides.org/assets/media/documents/pesticides/factsheets/Carbaryl1.pdf>). Accessed 1 March 2024.
- Carson R. 2002. *Silent Spring*. Houghton Mifflin Harcourt.
- Chang X, Heene E, Qiao F, Nick P. 2011. The phytoalexin resveratrol regulates the initiation of hypersensitive cell death in *Vitis* cell. *PLoS One* 6:e26405.
- Chen J, Zhang X, Rathjen JP, Dodds PN. 2022. Direct recognition of pathogen effectors by plant NLR immune receptors and downstream signalling. *Essays Biochem* 66:471–483.
- Chen L, Zhang L, Xiang S, Chen Y, Zhang H, Yu D. 2021. The transcription factor WRKY75 positively regulates jasmonate-mediated plant defense to necrotrophic fungal pathogens. *J Exp Bot* 72:1473–1489.

- Chong J, Le Henanff G, Bertsch C, Walter B. 2008. Identification, expression analysis and characterization of defense and signaling genes in *Vitis vinifera*. *Plant Physiol Biochem* 46:469–481.
- Ennis WB. 1948. Responses of Certain Plants to O-isopropyl N-phenyl Carbamate. University of Wisconsin--Madison.
- EPA. 2003. United States Environmental Protection Agency, Pesticides. Carbaryl. <https://archive.epa.gov/pesticides/chemicalsearch/chemical/foia/web/pdf/056801/056801-2003-10-30a.pdf>. Accessed 28 November 2023.
- EPA. 2004. United States Environmental Protection Agency, Carbaryl IRED Facts | US EPA ARCHIVE DOCUMENT. [https://archive.epa.gov/pesticides/reregistration/web/pdf/carbaryl\\_factsheet.pdf](https://archive.epa.gov/pesticides/reregistration/web/pdf/carbaryl_factsheet.pdf). Accessed 28 November 2023.
- EPA. 2015a. United States Environmental Protection Agency, Insecticides. <https://www.epa.gov/caddis/insecticides>. Accessed 28 November 2023.
- EPA. 2015b. United States Environmental Protection Agency, Pesticide Product Label, SEVIN SL CARBARYL INSECTICIDE, 10/21/2015. [https://www3.epa.gov/pesticides/chem\\_search/ppls/000432-01227-20151021.pdf](https://www3.epa.gov/pesticides/chem_search/ppls/000432-01227-20151021.pdf). Accessed 28 November 2023.
- Fenthion. PubChem. as found on the website (<https://pubchem.ncbi.nlm.nih.gov/compound/3346>). Accessed 28 November 2023
- Gambino G, Perrone I, Gribaudo I. 2008. A Rapid and effective method for RNA extraction from different tissues of grapevine and other woody plants. *Phytochem Anal* 19:520–525.

- Gao F, Shu X, Ali MB, Howard S, Li N, Winterhagen P, Qiu W, Gassmann W. 2010. A functional EDS1 ortholog is differentially regulated in powdery mildew resistant and susceptible grapevines and complements an Arabidopsis eds1 mutant. *Planta* 231:1037–1047.
- Giménez-Moolhuyzen M, Blom J van der, Lorenzo-Mínguez P, Cabello T, Crisol-Martínez E. 2020. Photosynthesis Inhibiting Effects of Pesticides on Sweet Pepper Leaves. *Insects* 11.
- Guo X, Wei F, Jian H, Lian B, Dang X, Yang M, Fu X, Ma L, Lu J, Wang H, et al. 2023. Systematic analysis of the NDR1/HIN1-like (NHL) family in *Gossypium hirsutum* reveals a role of GhNHL69 in responding to cold stress. *Ind Crops Prod* 206:117659.
- Haley CS, Knott SA. 1992. A simple regression method for mapping quantitative trait loci in line crosses using flanking markers. *Heredity* 69:315–324.
- Hasan M, Bae H. 2017. An Overview of Stress-Induced Resveratrol Synthesis in Grapes: Perspectives for Resveratrol-Enriched Grape Products. *Molecules* 22.
- Hassan ASM. 2019. Inorganic-based pesticides: a review article. *Egypt Sci J Pestic* 5:39–52.
- Heil M, Bostock RM. 2002. Induced systemic resistance (ISR) against pathogens in the context of induced plant defences. *Ann Bot* 89:503–512.
- Hoffman R, Capel P, Larson S. 2000. Comparison of pesticides in eight U.S. urban streams. *Environ Toxicol Chem* 19.
- Horiuchi Y, Kimura R, Kato N, Fujii T, Seki M, Endo T, Kato T, Kawashima K. 2003. Evolutional study on acetylcholine expression. *Life Sci* 72:1745–1756.
- Jansen RC, Stam P. 1994. High resolution of quantitative traits into multiple loci via interval mapping. *Genetics* 136:1447–1455.

- Jeon J, Kretschmann A, Escher BI, Hollender J. 2013. Characterization of acetylcholinesterase inhibition and energy allocation in *Daphnia magna* exposed to carbaryl. *Ecotoxicol Environ Saf* 98:28–35.
- Johnson GF. 1935. The Early History of Copper Fungicides. *Agric Hist* 9:67–79.
- Jones JDG, Vance RE, Dangl JL. 2016. Intracellular innate immune surveillance devices in plants and animals. *Science* 354.
- Koeppel DE, Cox JK, Malone CP. 1978. Mitochondrial heredity: a determinant in the toxic response of maize to the insecticide methomyl. *Science* 201:1227–1229.
- Lee S, Barron M. 2016. Mechanism-Based Analysis of Acetylcholinesterase Inhibitory Potency of Organophosphates, Carbamates, and Their Analogs.
- Lefevre H, Bauters L, Gheysen G. 2020. Salicylic Acid Biosynthesis in Plants. *Front Plant Sci* 11:338.
- Li J, Zhong R, Palva ET. 2017. WRKY70 and its homolog WRKY54 negatively modulate the cell wall-associated defenses to necrotrophic pathogens in *Arabidopsis*. *PLoS One* 12:e0183731.
- Lichtenstein EP, Millington WF, Cowley GT. 1962. Insecticide Effects on Plant Growth, Effect of Various Insecticides on Growth and Respiration of Plants. *J Agric Food Chem* 10:251–256.
- Lin Z, Zhang W, Pang S, Huang Y, Mishra S, Bhatt P, Chen S. 2020. Current Approaches to and Future Perspectives on Methomyl Degradation in Contaminated Soil/Water Environments. *Molecules* 25.

- Liu C, Peang H, Li X, Liu C, Lv X, Wei X, Zou A, Zhang J, Fan G, Ma G, et al. 2020. Genome-wide analysis of NDR1/HIN1-like genes in pepper (*Capsicum annuum* L.) and functional characterization of CaNHL4 under biotic and abiotic stresses. *Hortic Res* 7:93.
- Liu N, Xu Q, Zhu F, Zhang L. 2006. Pyrethroid resistance in mosquitoes. *Insect Sci* 13:159–166.
- Lorenzo O, Piqueras R, Sánchez-Serrano JJ, Solano R. 2003. ETHYLENE RESPONSE FACTOR1 Integrates Signals from Ethylene and Jasmonate Pathways in Plant Defense[W]. *Plant Cell* 15:165–178.
- Lu H. 2009. Dissection of salicylic acid-mediated defense signaling networks. *Plant Signal Behav* 4:713–717.
- Martin GB, Frary A, Wu T, Brommonschenkel S, Chunwongse J, Earle ED, Tanksley SD. 1994. A member of the tomato Pto gene family confers sensitivity to fenthion resulting in rapid cell death. *Plant Cell* 6:1543–1552.
- Morel JB, Dangl JL. 1997. The hypersensitive response and the induction of cell death in plants. *Cell Death Differ* 4:671–683.
- Moser VC. 2014. Fenthion. *In* *Encyclopedia of Toxicology*. pp. 583–585. Elsevier.
- Mount DW. 2007. Using the Basic Local Alignment Search Tool (BLAST). *CSH Protoc* 2007:db.top17.
- Paisley-Jones C. 2020. APPENDIX 1-4. Usage Data for Carbaryl – SUUM. United States Environmental Protection Agency.
- Pesticide Factsheets. Northwest Center for Alternatives to Pesticides. as found on the website ([https://www.pesticide.org/pesticide\\_factsheets](https://www.pesticide.org/pesticide_factsheets)). Accessed 29 February 2024.

- Pezet R, Gindro K, Viret O, Spring J-L. 2004. Glycosylation and oxidative dimerization of resveratrol are respectively associated to sensitivity and resistance of grapevine cultivars to downy mildew. *Physiol Mol Plant Pathol* 65:297–303.
- Polyrakis IT. 2009. Environmental Pollution from Pesticides. *In* Predictive Modeling and RiskAssessment. R Costa and K Kristbergsson (eds.), pp. 201–224. Springer US, Boston, MA.
- Purves D, Augustine GJ, Fitzpatrick D, Katz LC, LaMantia A-S, McNamara JO, Mark Williams S. 2001. Acetylcholine. Sinauer Associates.
- Radcliffe EB, Hutchison WD, Cancelado RE. 2009. Integrated Pest Management: Concepts, Tactics, Strategies and Case Studies. Cambridge University Press.
- Reddy D, Rao BN. 2002. Efficacy of Selected Insecticides against Pests of Grapevine. *Pesticide Research Journal*.
- Re-evaluation Decision RVD2016-02. 2016. Health Canada Pest Management Regulatory Agency.
- Rosado D, Ackermann A, Spassibojko O, Rossi M, Pedmale UV. 2022. WRKY transcription factors and ethylene signaling modify root growth during the shade-avoidance response. *Plant Physiol* 188:1294–1311.
- Rukavtsova EB, Alekseeva VV, Tarlachkov SV, Zakharchenko NS, Ermoshin AA, Zimnitskaya SA, Surin AK, Gorbunova EY, Azev VN, Sheshnitsan SS, et al. 2022. Expression of a Stilbene Synthase Gene from the *Vitis labrusca* x *Vitis vinifera* L. Hybrid Increases the Resistance of Transgenic *Nicotiana tabacum* L. Plants to *Erwinia carotovora*. *Plants* 11.

- Shakir SK, Irfan S, Akhtar B, Rehman SU, Daud MK, Taimur N, Azizullah A. 2018. Pesticide-induced oxidative stress and antioxidant responses in tomato (*Solanum lycopersicum*) seedlings. *Ecotoxicology* 27:919–935.
- Sinha M, Singh RP, Kushwaha GS, Iqbal N, Singh A, Kaushik S, Kaur P, Sharma S, Singh TP. 2014. Current overview of allergens of plant pathogenesis related protein families. *ScientificWorldJournal* 2014:543195.
- Spoel SH, Koornneef A, Claessens SMC, Korzelius JP, Van Pelt JA, Mueller MJ, Buchala AJ, Métraux J-P, Brown R, Kazan K, et al. 2003. NPR1 modulates cross-talk between salicylate- and jasmonate-dependent defense pathways through a novel function in the cytosol. *Plant Cell* 15:760–770.
- Stroud EA, Jayaraman J, Templeton MD, Rikkerink EHA. 2022. Comparison of the pathway structures influencing the temporal response of salicylate and jasmonate defence hormones in *Arabidopsis thaliana*. *Front Plant Sci* 13:952301.
- Tan W-J, Xiao S, Chen Q-F. 2015. Potential role of salicylic acid in modulating diacylglycerol homeostasis in response to freezing temperatures in *Arabidopsis*. *Plant Signal Behav* 10:e1082698.
- Tudi M, Daniel Ruan H, Wang L, Lyu J, Sadler R, Connell D, Chu C, Phung DT. 2021. Agriculture Development, Pesticide Application and Its Impact on the Environment. *Int J Environ Res Public Health* 18.
- Umetsu N, Shirai Y. 2020. Development of novel pesticides in the 21st century. *J Pestic Sci* 45:54–74.
- US Geological Survey. 2024. Estimated Annual Agricultural Pesticide Use. as found on the website

- ([https://water.usgs.gov/nawqa/pnsp/usage/maps/show\\_map.php?year=2018&map=CARBARYL&hilo=L](https://water.usgs.gov/nawqa/pnsp/usage/maps/show_map.php?year=2018&map=CARBARYL&hilo=L)). Accessed 29 February 2024.
- van Verk MC, Bol JF, Linthorst HJM. 2011. WRKY transcription factors involved in activation of SA biosynthesis genes. *BMC Plant Biol* 11:89.
- Voorrips RE. 2002. MapChart: software for the graphical presentation of linkage maps and QTLs. *J Hered* 93:77–78.
- Wang M, Vannozzi A, Wang G, Liang Y-H, Tornielli GB, Zenoni S, Cavallini E, Pezzotti M, Cheng Z-MM. 2014. Genome and transcriptome analysis of the grapevine (*Vitis vinifera* L.) WRKY gene family. *Hortic Res* 1:14016.
- Wang N, Song N, Tang Z, Wang X, Kang Z, Dai L, Wang B. 2020. Constitutive Expression of Arabidopsis Senescence Associated Gene 101 in *Brachypodium distachyon* Enhances Resistance to *Puccinia brachypodii* and *Magnaporthe oryzae*. *Plants* 9.
- Ware D. 2007. Gramene. *Methods Mol Biol* 406:315–329.
- Weber E, Benedictis JD, Smith RJ, Granett J. 1996. Enzone does little to improve health of phylloxera-infested vineyards. *Calif Agric* 50:19–23.
- Yamazaki A, Battenberg K, Shimoda Y, Hayashi M. 2022. NDR1/HIN1-Like Protein 13 Interacts with Symbiotic Receptor Kinases and Regulates Nodulation in *Lotus japonicus*. *Mol Plant Microbe Interact* 35:845–856.
- Zeng ZB. 1994. Precision mapping of quantitative trait loci. *Genetics* 136:1457–1468.
- Zhou J-M, Zhang Y. 2020. Plant Immunity: Danger Perception and Signaling. *Cell* 181:978–989.



**Table 1.** Major types of insecticides with respective modes of action and pest targets (EPA 2015a)

Insecticide Type	Mode of Action	Pest Target
Organochloride	Act through sodium/potassium imbalance or inhibit GABA	Broad-range
Organophosphate	Acetylcholinesterase inhibition	Broad-range
Organosulfur	Ovicidal	Mites
Carbamates	Acetylcholinesterase inhibition	Broad-range
Formamidines	Inhibit monoamine oxidase	Broad-range against organophosphate- and carbamate-resistant pests
Dinitrophenols	Inhibit oxidative phosphorylation and ATP production	Wide range of insects
Organotins	Inhibit oxidative phosphorylation and ATP production	Mites, mollusks
Pyrethroids	Inhibit inter-membrane sodium channel regulation	Insects and fish
Nicotinoids	Irreversibly block acetylcholine receptors	Specific insects
Spinosyns	Disrupt acetylcholine regulation	Specific insects
Pyrazoles	Disrupt ATP formation	Specific insects
Pyridazinones	Inhibit mitochondrial electron transport	Mites, aquatic arthropods, fish
Quinazolines	Inhibit chitin synthesis	Wide range of insects
Antibiotics	Inhibit GABA	Specific insects
Benzoylureas	Interfere with chitin synthesis	Specific insect and fish larvae

**Table 2.** Scale used to score leaf disks in the *in vitro* carbaryl sensitivity bioassay. A score of 1 indicates insensitivity; a score greater than 1 indicates sensitivity and its degree.

Score	Symptoms
1	No change
2	Discoloration, no obvious necrosis
3	Obvious necrosis covering approximately 25-45% of the leaf
4	Approximately 50% necrosis
5	Approximately 55-64% necrosis
6	Approximately 65-70% necrosis
7	Approximately 75% necrosis (perimeter of disk is unaffected)
8	Entire interior is affected (perimeter of disk is unaffected)
9	Entire leaf disk affected (100% necrosis)

**Table 3.** F1 hybrid plants used for RT-qPCR analysis. Hpt: hours post-treatment. The 0 hpt sample was used as an untreated control.

Samples					
Sensitive Individuals (hpt)			Insensitive Individuals (hpt)		
E16 (0)	E49 (0)	E69 (0)	E112 (0)	E183 (0)	E222 (0)
E16 (24)	E49 (24)	E69 (24)	E112 (24)	E183 (24)	E222 (24)
E16 (48)	E49 (48)	E69 (48)	E112 (48)	E183 (48)	E222 (48)
E16 (72)	E49 (72)	E69 (72)	E112 (72)	E183 (72)	E222 (72)

**Table 4.** Summary of sequencing data obtained for the control (0-hour), 24-, 48-, or 72-hours post-treatment in insensitive (IN) and sensitive (SE) RNA-seq experiments. The total number of reads is listed for each of the three technical replicates for each treatment and time point.

Hours Post-Treatment	# of Reads	Hours Post-Treatment	# of Reads
IN 00-A	127,122,550	SE 00-A	118,187,520
IN 00-B	125,595,774	SE 00-B	127,752,048
IN 00-C	123,712,116	SE 00-C	130,517,366
IN 24-A	117,053,478	SE 24-A	125,806,264
IN 24-B	123,901,204	SE 24-B	111,726,222
IN 24-C	131,850,694	SE 24-C	117,911,238
IN 48-A	126,497,772	SE 48-A	118,345,500
IN 48-B	122,395,020	SE 48-B	110,982,884
IN 48-C	114,568,440	SE 48-C	107,355,028
IN 72-A	139,030,984	SE 72-A	97,759,296
IN 72-B	123,538,420	SE 72-B	122,964,140
IN 72-C	118,341,622	SE 72-C	113,534,014

**Table 5.** The number of genes with two- or four-fold change in expression relative to untreated control at 24-, 48-, and 72-hours post-treatment (hpt) with carbaryl.

	Sample	hpt <sup>#</sup>	Number of DEGs* Relative to Control		
			Upregulated	Downregulated	Total
2-fold Regulated Genes	IN	24	2,380	717	3,097
		48	2,436	1,055	3,491
		72	1,958	2,473	4,431
	SE	24	3,005	1,132	4,137
		48	2,410	633	3,043
		72	2,245	3,187	5,432
4-fold Regulated Genes	IN	24	584	113	697
		48	589	174	763
		72	328	612	940
	SE	24	477	72	549
		48	427	33	460
		72	538	552	1090

\*Differentially expressed gene

<sup>#</sup>Hours post-treatment

**Table 6.** Differentially expressed genes (DEGs) that were identified via RNA-seq analysis based on 4-fold up- or down-regulation relative to 0 hours post-treatment (control) at FDR-adjusted  $p < 0.01$ . Genes were categorized by biological function using **Gene Ontology Resource** at <https://geneontology.org/>.

Description (BLAST, <i>Vitis</i> )	Gene ID	Pathway Involvement	Response Group
<i>AAA-ATPase ASD</i>	Vitvi14g01840	SA, JA	SE
Cytochrome p450	Vitvi07g01657	SA, JA	SE
Cytokinin dehydrogenase 3	Vitvi11g01371	SA	SE and IN
Dirigent protein 22	Vitvi17g00450	SA, JA	SE
EDS1	Vitvi17g01520	SA, JA	SE and IN
Ethylene-response transcription factor C3	Vitvi05g00715	JA	SE and IN
Heat stress transcription factor	Vitvi08g01931	JA	SE
Major allergen PR-1	Vitvi05g00071	SA, JA	SE
Major strawberry allergen PR-10	Vitvi05g01759	SA, JA	SE
Pectinesterase 2	Vitvi15g00704	SA	SE and IN
NDR1/HIN1-like protein 6	Vitvi04g00764	SA, JA	SE
Peroxidase 73	Vitvi07g01614	SA, JA	SE
Senescence-associated carboxylesterase 101 (SAG101)	Vitvi14g03032	SA	SE and IN
Senescence-induced receptor-like serine/threonine-protein kinase MYB15	Vitvi09g01555	SA, JA	SE
MYB15	Vitvi05g01733	JA	SE and IN
MYB62	Vitvi17g00309	SA, JA	SE and IN
WRKY75	Vitvi01g01680	SA, JA	SE and IN
Shikimate dehydrogenase	Vitvi05g00715	SA	SE and IN
Shikimate dehydrogenase	Vitvi14g00340	SA	SE and IN
Shikimate kinase/chorismate	Vitvi18g01517	SA	SE and IN
Trans-resveratrol di-O-methyltransferase	Vitvi12g02245	SA, JA	SE
Stilbene synthase	Vitvi16g01485	SA, JA	SE and IN

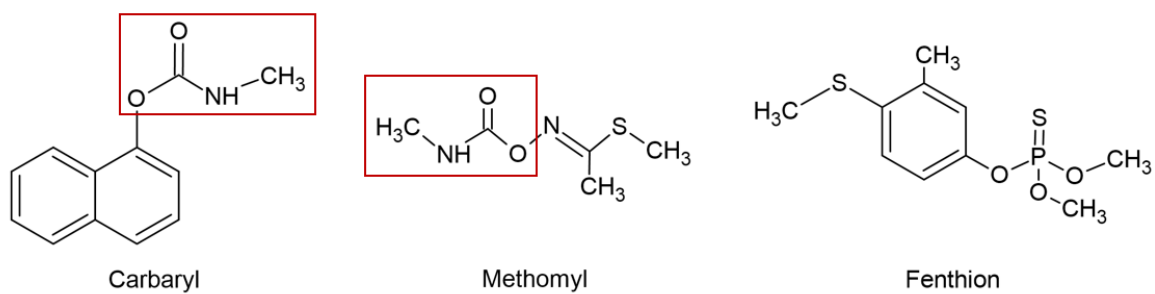


**Figure 1.** Molecular structure of three insecticide compounds that have been reported for their effect in certain plant genotypes. The framed molecular component of carbaryl and methomyl represent the carbamate moiety (ChemSketch, version 2023.1.2, Advanced Chemistry Development, Inc. (ACD/Labs), Toronto, ON, Canada, [www.acdlabs.com](http://www.acdlabs.com)).

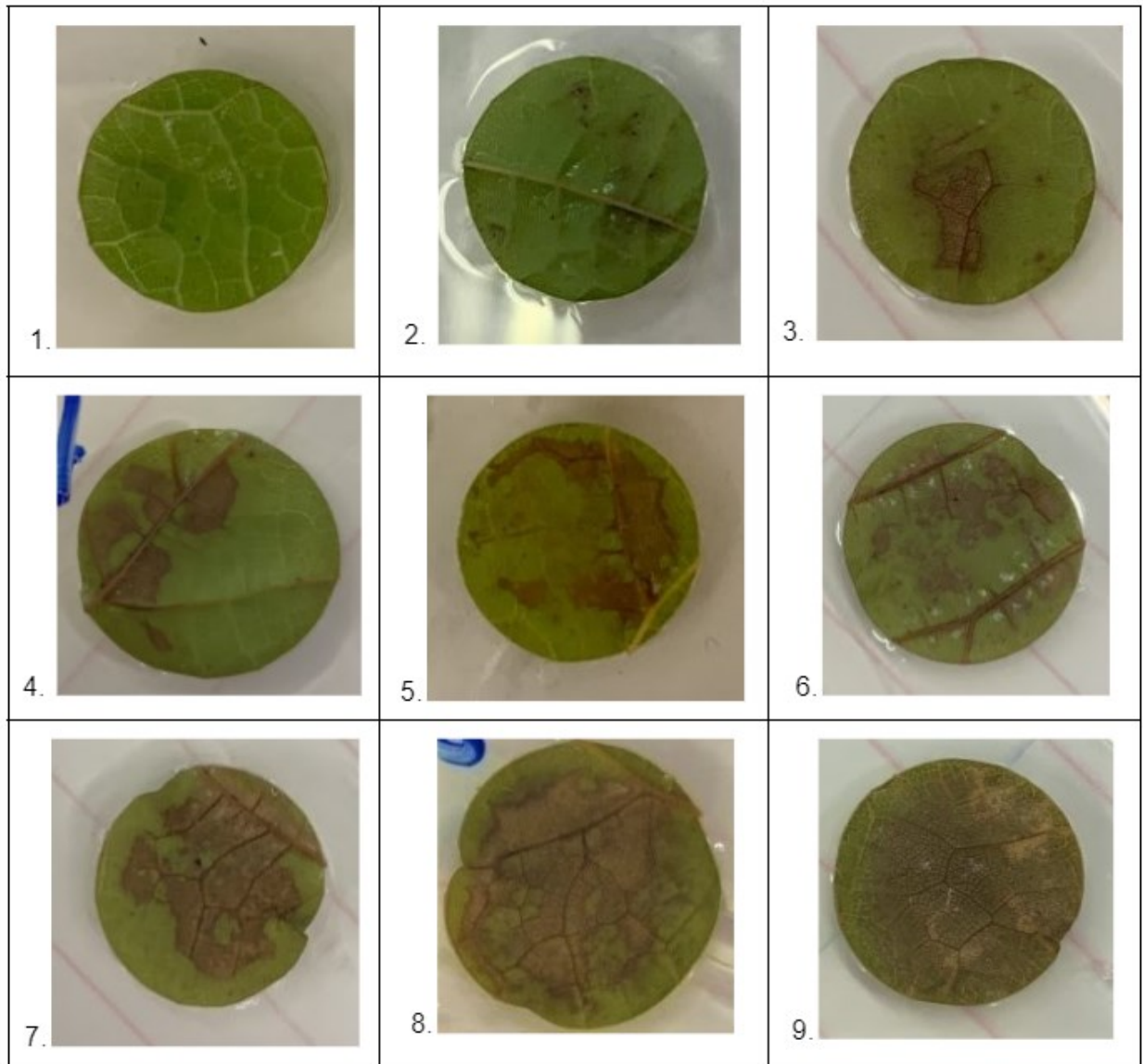


**Figure 2.** Leaf disks used as representatives for each score in the *in vitro* carbaryl sensitivity bioassay. Leaf disks were submerged in Sevin SL suspension at 0.53% concentration.



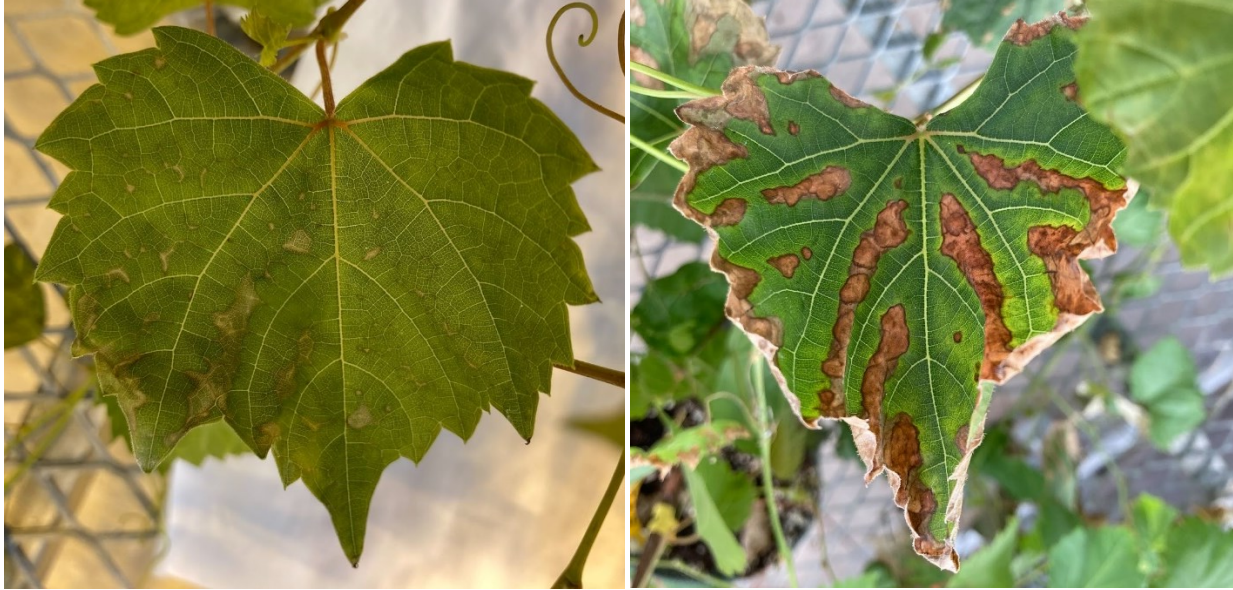


**Figure 3.** Leaf of a carbaryl-treated sensitive vine 3 days (**left**) and 21 days (**right**) following treatment in the greenhouse. Vines were sprayed with Sevin SL suspension at 0.53% concentration, which corresponds to 50x the concentration recommended by the manufacturer for field application.



**Figure 4.** Leaf of a carbaryl-treated sensitive vine 17 days following treatment in the field. Vines were sprayed with a 0.0106% Sevin SL suspension, which corresponds to the concentration recommended by the manufacturer for field application.

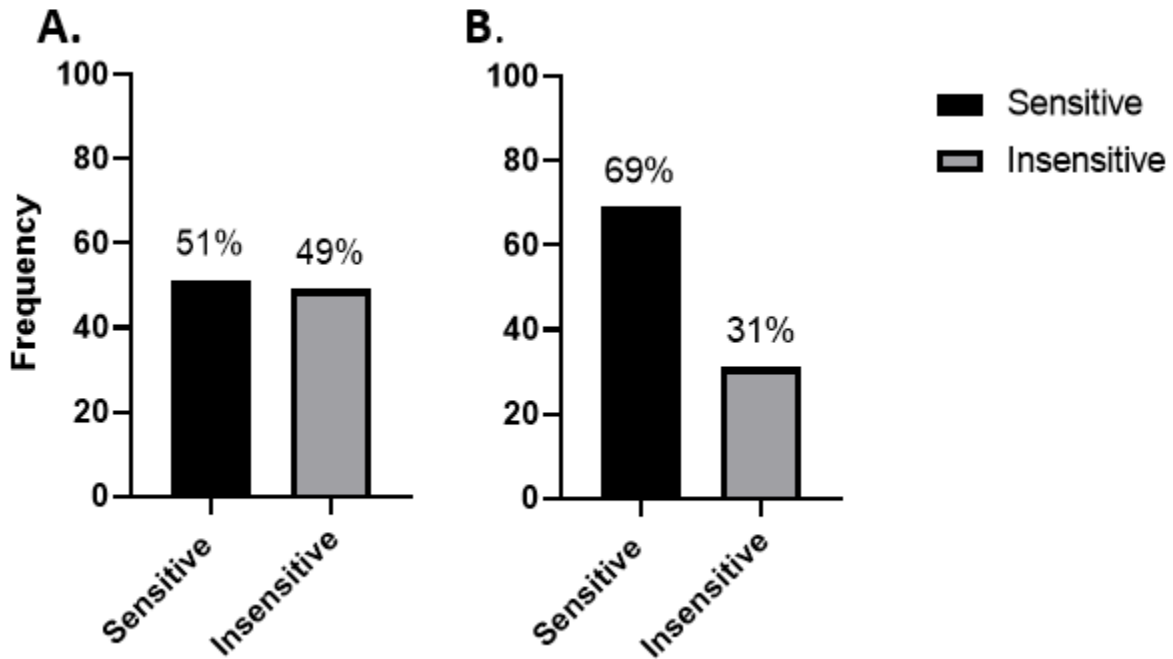


**Figure 5.** Segregation of the carbaryl sensitivity phenotype in different environments. Percent of carbaryl-sensitive and insensitive F1 hybrid vines in (A) NY and (B) MO. The difference in segregation across NY and MO vineyards could be explained by the imperfect concordance between vines at both locations, different individuals performing phenotyping at the two locations, or the yet-undetermined influence of environmental factors on the observed phenotype.

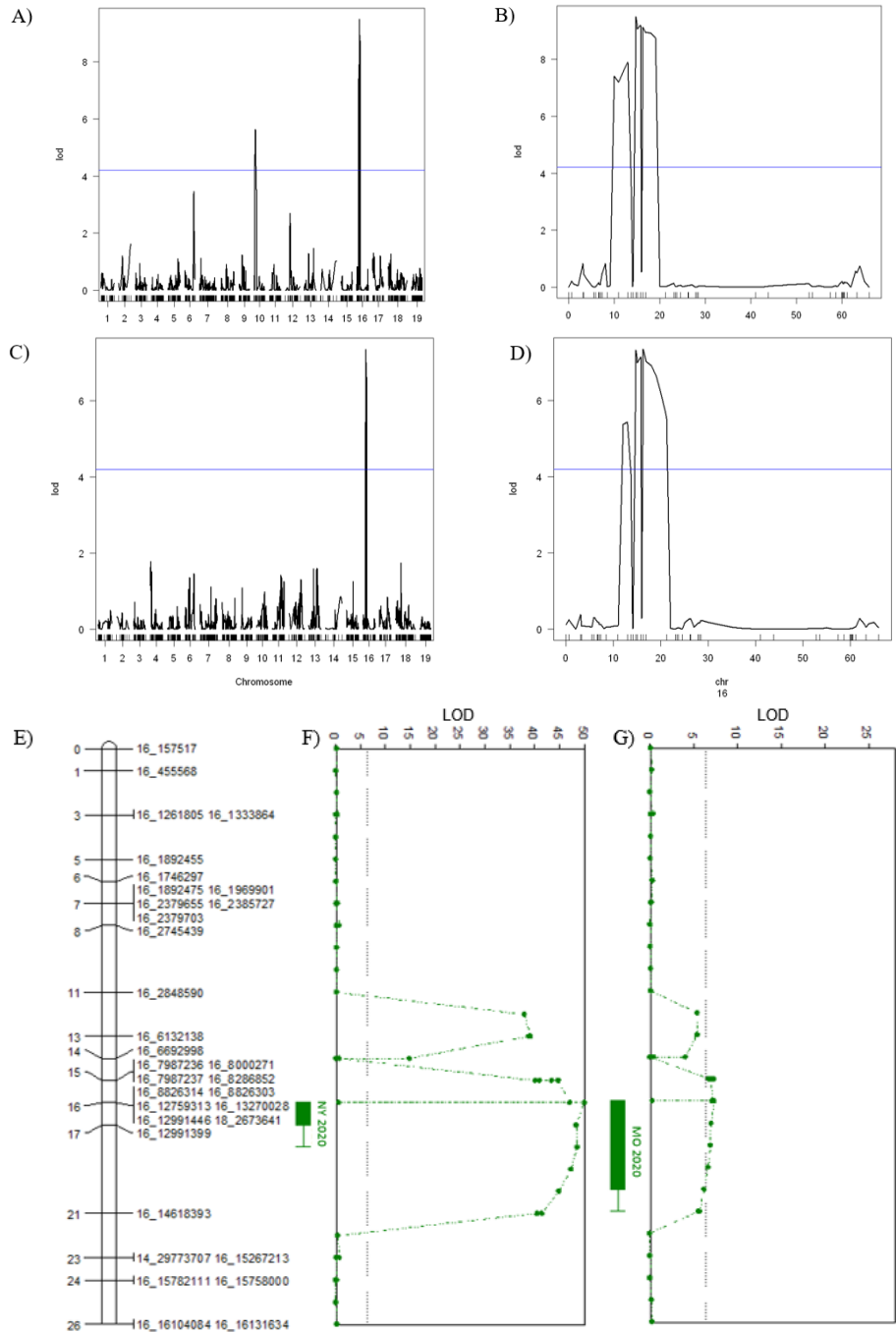


**Figure 6.** Quantitative trait locus (QTL) graphs plotting genome position versus the logarithm of odds (LOD) for the carbaryl-sensitivity allele in hybrid grapevines. The position of a major QTL peak was detected by mapping field phenotype data of a replicated F1 progeny in (A and B) NY and (C and D) MO. A and C, QTL position mapped to the entire genome, B and D, QTL position mapped to chromosome 16 only. E, Linkage map of the 0 to 26-cM region of chromosome 16. F and G, LOD graph of QTL peaks mapped in NY and MO, respectively. Solid bars and whiskers represent QTL positions' 95% and 99% confidence intervals.

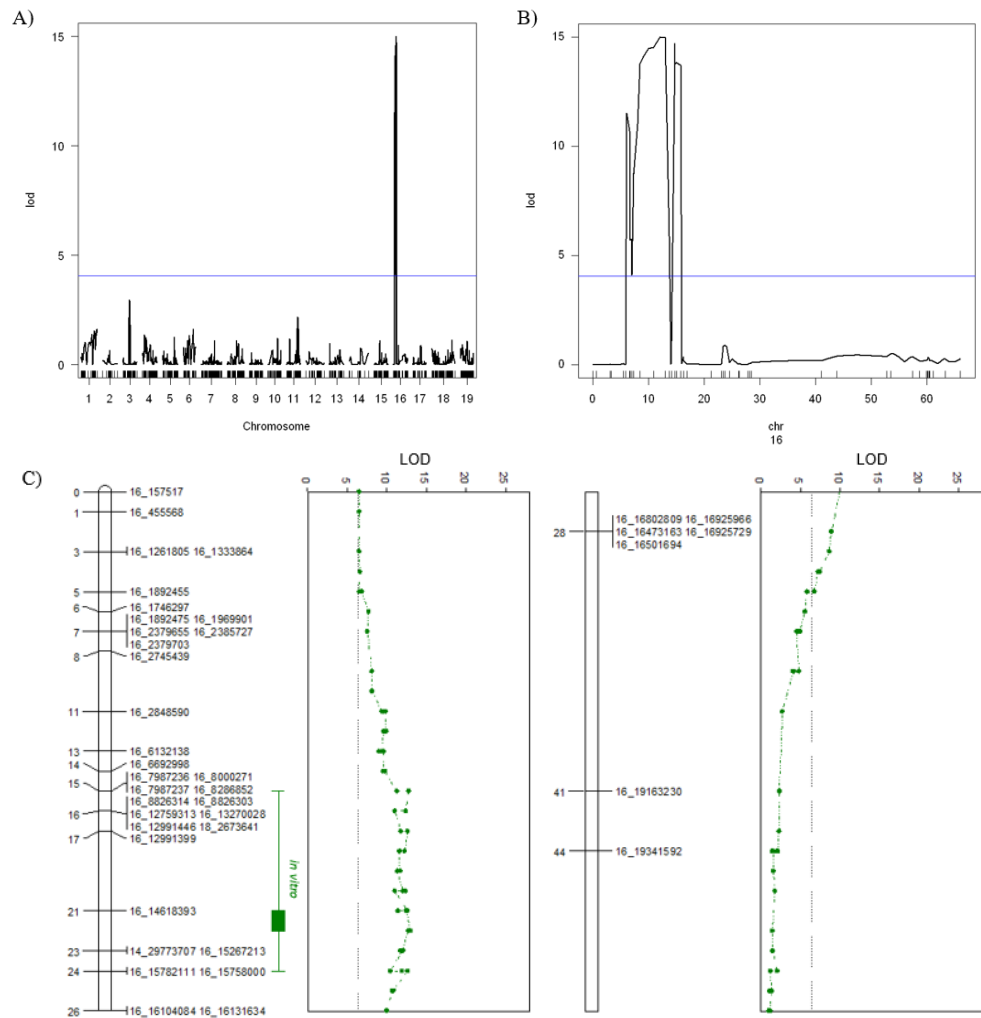


**Figure 7.** Quantitative trait locus (QTL) and logarithm of odds (LOD) graphs of the carbaryl-sensitivity allele in *Vitis*. The QTL position was determined using (A and B) a leaf disk bioassay in F1 progeny, which resulted in a significant peak on chromosome 16 of the seed parent (*V. rupestris*). (C) Linkage map of the top 50-cM region of chromosome 16.

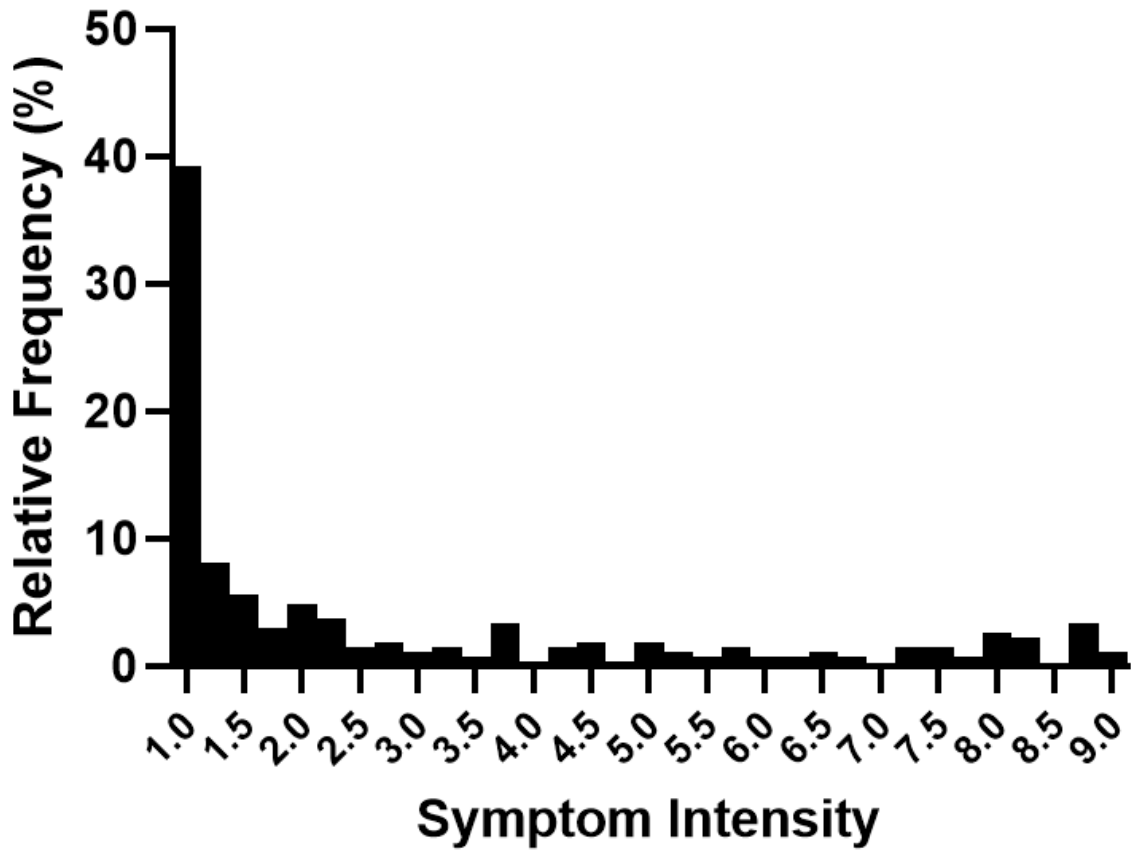


**Figure 8.** Frequency of distribution of leaf disks with various symptom intensity scores.

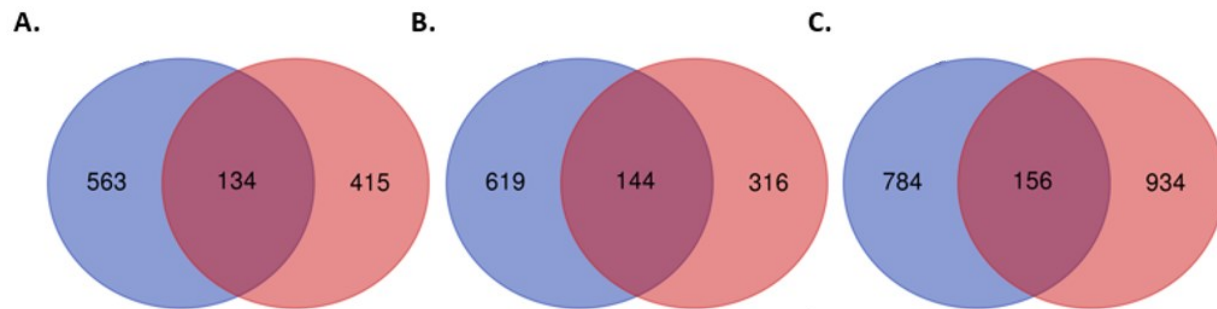


**Figure 9.** Number of carbaryl-responsive genes four times up- or down-regulated unique to and shared between sensitive and insensitive vines. **A**, **B**, and **C** show the number of differentially expressed genes at 24-, 48-, or 72-hours post-treatment (hpt), respectively. Differentially expressed genes (DEGs) are those that were 4-fold up- or down-regulated at false discovery rate (FDR)-adjusted  $p < 0.05$ . Blue and red areas of the Venn diagram indicate insensitive and sensitive plants, respectively.

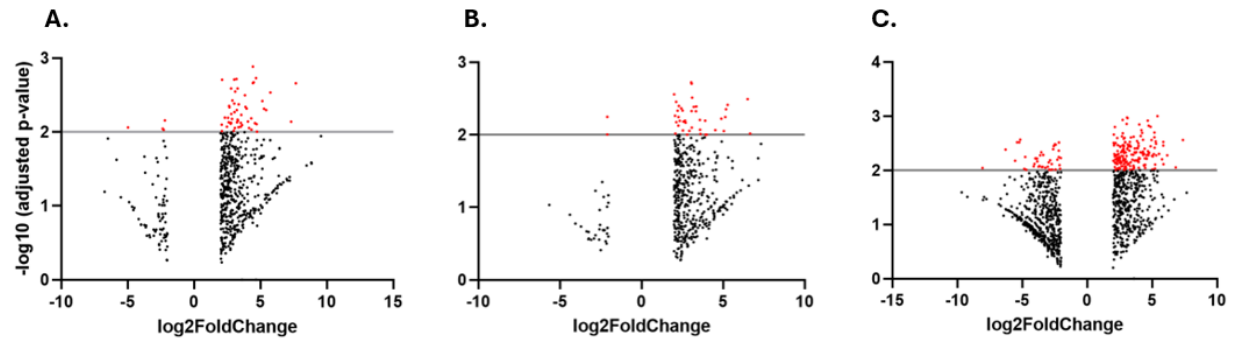


**Figure 10.** Genes with a log<sub>2</sub> fold-change of < -2 or > +2 in expression at 24-, 48-, or 72-hours post-treatment (hpt) (**A**, **B**, and **C**, respectively). Red dots denote genes with the FDR-adjusted p-value of  $\leq 0.01$ .



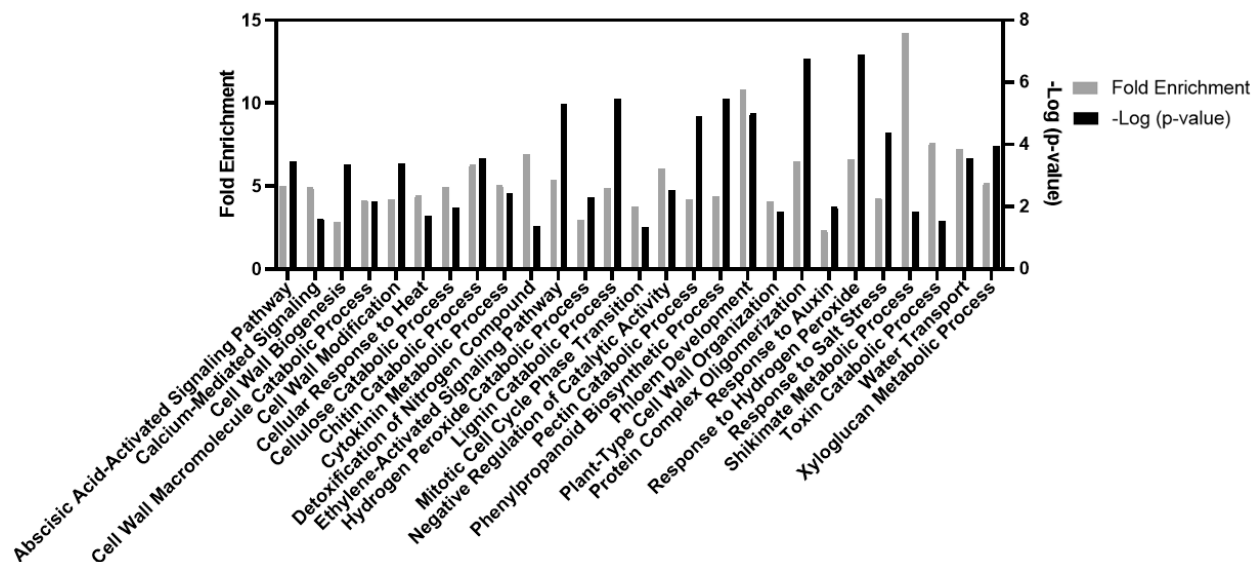


**Figure 11.** Gene ontology (GO) enrichment analysis of genes that were four-fold up- or downregulated in sensitive (SE) plants at 24-, 48-, or 72-hours post-treatment (hpt). Biological processes were assessed using a p-value < 0.05 and a fold enrichment > 2.0.

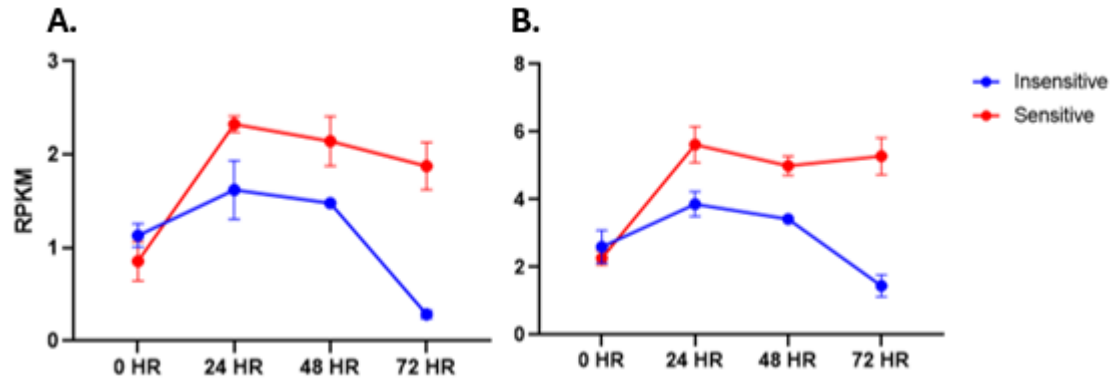


**Figure 12.** Expression of key regulatory genes *EDS1* and *SAG101* (A and B, respectively) of the SA-mediated defense pathway in carbaryl-sensitive and insensitive F1 hybrid vines. Normalized transcript levels (reads per kilobase per million reads mapped [RPKM]) in control (0-hour) and at 24-, 48-, and 72-hours post-treatment (hpt).

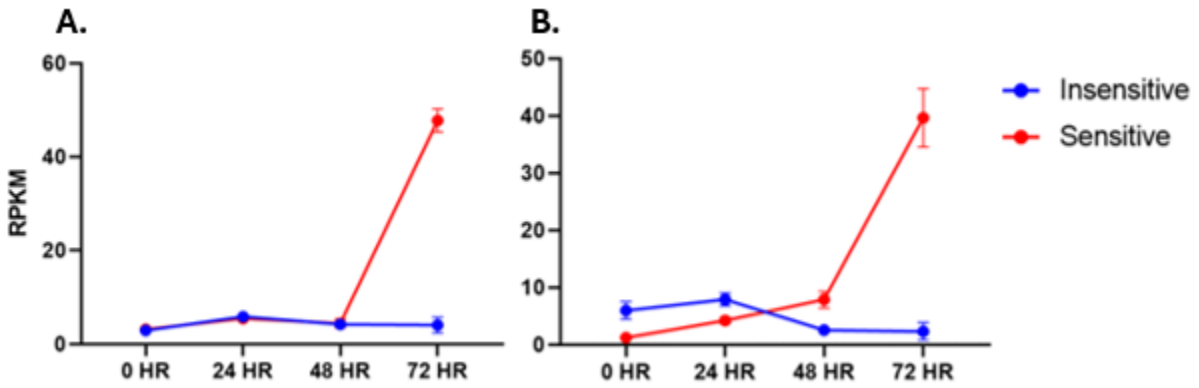


**Figure 13.** Expression of *trans-resveratrol di-O-methyltransferase* and *stilbene synthase 2* (A and B, respectively) in carbaryl-sensitive and insensitive F1 hybrid vines . Normalized transcript levels (reads per kilobase per million reads mapped [RPKM]) in control (0-hour) and at 24-, 48-, and 72-hours post-treatment (hpt).

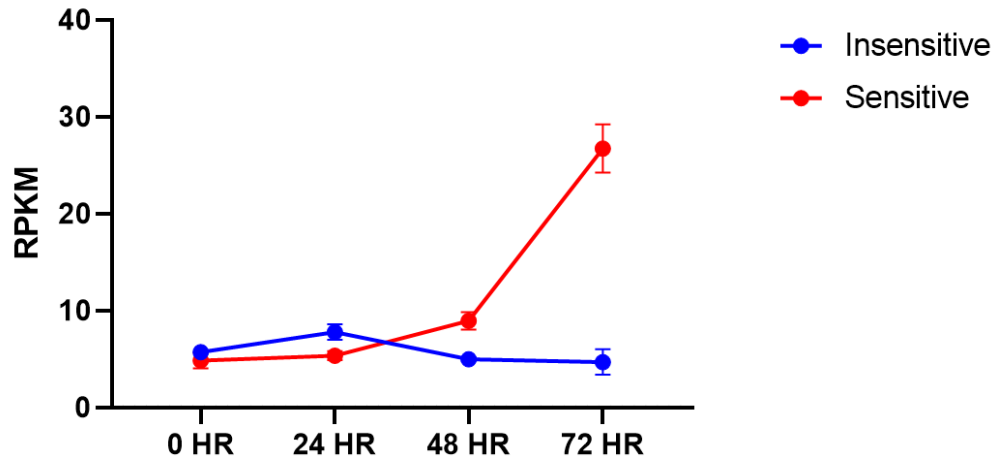


**Figure 14.** Expression of *NDR1/HIN1-like protein 6 (NHL6)* in carbaryl-sensitive and insensitive F1 hybrid vines. Normalized transcript levels (reads per kilobase per million reads mapped [RPKM]) in control (0-hour) and at 24-, 48-, and 72-hours post-treatment (hpt).

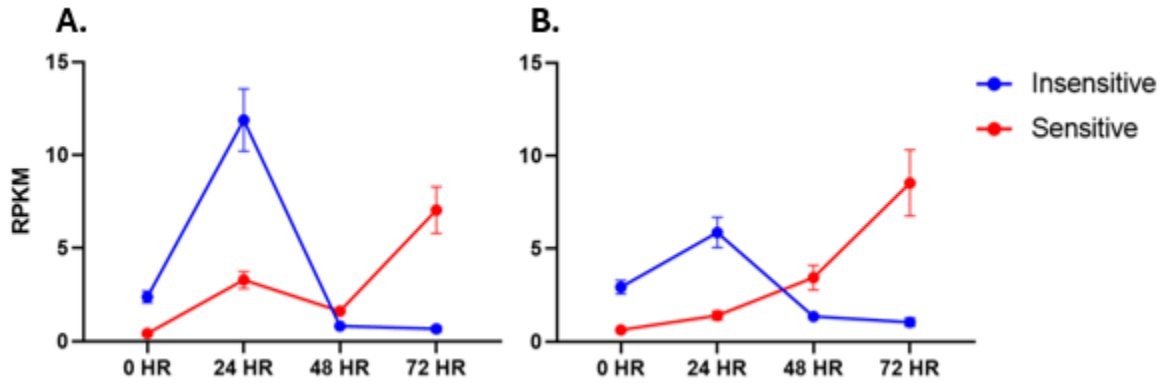


**Figure 15.** Expression levels of the regulatory genes *ethylene-response factor C3* and *jasmonate-induced oxygenase 1* (A and B, respectively) of the JA- and ETH-mediated defense pathway in caribaryl-sensitive and -insensitive F1 hybrid vines. Normalized transcript levels (reads per kilobase per million reads mapped [RPKM]) in control (0-hour) and at 24-, 48-, and 72-hours post-treatment (hpt).

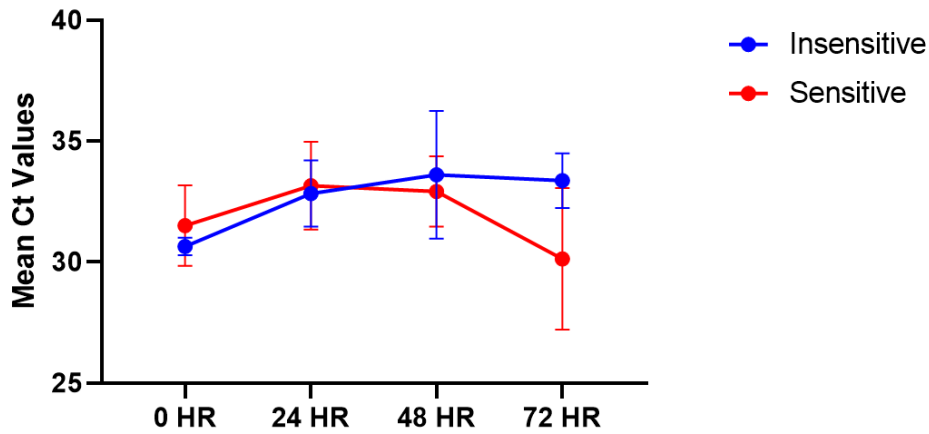


**Figure 16.** Expression of *NDR1/HIN1-like protein 6 (NHL6)* in carbaryl-sensitive and insensitive F1 hybrid vines measured by RT-qPCR. Transcript levels are expressed as mean cycle number at threshold ( $C_t$ ) in three sensitive and three insensitive individual vines at control (0-hour) and at 24-, 48-, and 72-hours post-treatment (hpt).